Reprogramming of the cardiac phosphoproteome in conjunction with proteome and transcriptome creates the enhanced performance and protection circuitry in response to chronic adenylyl cyclase-driven stress

Jia-Hua Qu, Khalid Chakir, Kirill V. Tarasov, Daniel R. Riordon, Maria Grazia Perino, Allwin Jennifa Silvester, and Edward G. Lakatta *

Laboratory of Cardiovascular Science, Intramural Research Program, National Institute on Aging, National Institutes of Health, Baltimore, MD 21224, USA.

Address correspondence to:

Dr. Edward G. Lakatta*

Laboratory of Cardiovascular Science

Intramural Research Program

National Institute on Aging

National Institutes of Health

251 Bayview Boulevard

Suite 100

Baltimore, MD 21224

USA.

Tel: +1 410-558-8202

lakattae@grc.nia.nih.gov

Abstract

Our previous work demonstrated the existence of a remarkable adaptive paradigm of heart performance and protection in response to the constitutive challenge of marked cardiac-specific overexpression of adenylyl cyclase type 8 (TGAC8). However, the molecular regulatory mechanisms remain elusive due to the superficial analysis of transcriptome and proteome. Because PKA signaling is the predominantly activated pathway in the TGAC8 left ventricle (LV) performance and protection circuitry and phosphorylation related pathways were enriched from transcriptome and proteome, we hypothesized that phosphorylation states of numerous proteins are reprogrammed in pathways where the transcriptome and proteome were activated in TGAC8 vs. WT. We conducted an unbiased phosphoproteomics analysis in order to determine the role of altered protein phosphorylation in the chronic adaptive heart performance and protection profile of adult TGAC8 LV at 3-4 months of age, and integrated the phosphoproteome with transcriptome and proteome. Based on differentially regulated phosphoproteins by genotype, numerous stress-response pathways within reprogrammed TGAC8 LV, including PKA signaling, PI3K signaling, and AMPK signaling, predicted upstream regulators, e.g., PDPK1, PAK1 and PTK2B, and downstream functions, e.g., cell viability, protein quality control, and metabolism were enriched. In addition to PKA, numerous other kinases (83) and phosphatases (30) were hyper-phosphorylated in TGAC8 vs. WT. Hyper-phosphorylated transcriptional factors in TGAC8 were associated with increased mRNA transcription, and immune responses and metabolism pathways. Combination of the phosphoproteome with its proteome and with the previously published TGAC8 transcriptome enabled the elucidation of which cardiac performance and adaptive protection profiles were coordinately regulated at post-translational modification (PTM) (phosphorylation), translational and transcriptional levels. Many stress-response signaling pathways, i.e., PI3K/AKT, ERK/MAPK and ubiquitin labeling, were consistently enriched at transcriptional, translational and PTM levels, and that PI3K/AKT and ERK/MAPK signaling pathways were also activated in the TGAC8 LV. We verified some results through wet lab experiments. Thus, PTM of protein by phosphorylation, per se, contributes immensely to the heart performance and protection profile of TGAC8 LV, and is coordinately regulated with altered transcription and translation in the TGAC8 to activate critical stress-response pathways.

Keywords

left ventricle, adenylyl cyclase 8, AC-cAMP-PKA-Ca^{2+} signaling, phosphoproteome, proteome, transcriptome, PI3K/AKT signaling pathway.

Introduction

Cyclic AMP (cAMP) is a pivotal second messenger, which exerts multifaceted effects on most significant physiological processes, such as cardiac contractility, glycogenolysis and lipolysis, hormone release, etc[1]. In mammalians, there are nine transmembrane adenylyl cyclase (AC) (mAC) isoforms (AC1-9) and one soluble AC (sAC, also called AC10) catalyzing the conversion

of ATP into cAMP[2], which usually activates the phosphorylation cascade, serving as the central motif of cellular signaling[1,3]. Increased AC-cAMP-PKA-Ca^{2+} signaling is the quintessential component of both acute and chronic cardiac responses.

AC8, the isoform, is highly expressed in brain regions[2,4]. Unlike two dominant cardiac AC isoforms, AC5 and AC6, which are inhibited by intracellular Ca^{2+} and inhibited in heart failure (HF), AC8 is stimulated by Ca^{2+}-calmodulin (CM)[5,6] and involved in nervous system functions, like learning and memory[2,4]. Our lab and others have demonstrated that cardiac-specific overexpression of AC8 (TGAC8) markedly increases the heart rate and ejection fraction, similar to acute exercise but chronic and in the absence of corporal exertion, and persists on a 24 hours per day and 7 days per week basis[5,7-9]. Despite this persistent high-level of heart performance driven by markedly elevated level of AC8-cAMP-PKA-Ca^{2+} signaling, which usually proceeds to near-term cardiac dysfunction, the TGAC8 survives for an extended period of time, up to about a year of age without excessive mortality.

It is of utmost importance to unravel how the TGAC8 adapts the heart to this chronic stress, as this knowledge can be applied to the study of cardiac physiology and pathology and even to develop treatments for cardiovascular diseases (CVDs). In this regard, as a first "port-of-call", we had recently compared the LV transcriptome and proteome in TGAC8 and WT littermates[10]. Because PKA signaling pathway was highly enriched in TGAC8 vs. WT, we reasoned that protein phosphorylation will differ between TGAC8 and WT, and the phosphorylation modification will play a crucial role in the remarkable adaptation capacity of the TGAC8 heart in response to markedly increased AC8-cAMP-PKA-Ca^{2+} signaling. We have assessed the concordance of the genotypic differences at the phosphorylation level to some degree in western blot (WB) experiments[10].

As the body is a quite complex system, regulation at a single level cannot reveal the whole picture in an organism, and multiple levels of regulatory mechanisms are coordinated to defend against stimuli and maintain health[11]. Phosphorylation is one of the most important and most extensively studied post-translational modifications (PTMs) on proteins. Various kinases and phosphatases within cells phosphorylate and dephosphorylate a myriad of proteins respectively to regulate their activities and affect multiple signaling pathways. In the present research, we conducted Tandem Mass Tag (TMT)-labeling MS of left ventricular samples of the three-month old male TGAC8 and WT mice, to unravel the reprogrammed phosphoproteome and proteome of the TGAC8 left ventricle (LV). In addition, by comparing genotypic differences in the proteome and phosphoproteome of the present study with genotypic differences in transcriptome published previously[10], we sought to determine whether some adaptive mechanisms that emerge in the TGAC8 LV are regulated at transcriptional, translational and PTM (phosphorylation) levels.

Materials and Methods

1. Animals.

The cardiac-specific overexpression of AC8 (TGAC8) mouse, generated by inserting a cDNA coding for human AC8 after the murine α-myosin heavy chain promoter, was a gift from Nicole Defer/Jacques Hanoune, Unite de Recherches, INSERM U-99, Hôpital Henri Mondor, F-94010 Créteil, France. The 12-week old male TGAC mice were used as study cases, and age matched WT littermates, in the C57/BL6 background, were used as controls. All studies were performed in accordance with the Guide for the Care and Use of Laboratory Animals published by the National Institutes of Health (NIH Publication no. 85-23, revised 1996). The experimental protocols were approved by the Animal Care and Use Committee of the National Institutes of Health (protocol #441-LCS-2016).

2. Isolate and store mouse heart.

Three-month old male C57 mice (TGAC8 and WT) were euthanized and the heart was isolated. The left ventricle (LV) tissues were extracted and stored in tubes at -80°C.

3. Mass spectrometry for phosphoproteome and data process.

Four TGAC8 LVs and five WT LVs were sent to National Heart, Lung, and Blood Institute, National Institutes of Health, Bethesda to conduct mass spectrometry using the standard tandem mass tag (TMT) labeling method to obtain the phosphoproteome and total proteome concurrently in the same platform. The raw data were processed in Proteome Discover (ThermoFisher Scientific, software version 2.2). After filtering low quality signal, we remained the medium and high confidence peptides. For total proteins and phosphoproteins, we combined peptides to compute the normalized/standardized expressions with the default parameters. Then we divided the expressions of phosphoproteins to those of total proteins to obtain the normalized phosphoproteome. As the expressions appeared to be near normal distribution, we calculated the fold change by dividing the average value of TGAC8 samples by the average value of WT samples, and calculated p-value using two-sided unpaired Student's t-test.

4. Analyses of the TGAC8 LV transcriptome.

The processed transcriptomic data were obtained from our recently published work[10]. The significantly changed mRNAs (TGAC8 vs. WT, q-value < 0.05) were uploaded into DAVID[2] (version: 6.8; https://david.ncifcrf.gov/home.jsp) for Gene Ontology (GO) term enrichments, and were also imported into Ingenuity Pathway Analysis[3] (IPA (QIAGEN, March 2020)) for upstream kinases and phosphatases prediction. Kinases and phosphatases were selected from the

132 transcriptome and their changes at mRNA level were displayed to observe their regulation by the
133 overexpression of AC8.

134

135 **5. Analyses of phosphoproteome and proteome.**

136 Both unnormalized and normalized phosphoproteome were analyzed and visualized in PCA,
137 heatmap, and volcano plots. With the cutoff -log(p-value) > 1.3 and absolute(log2(fold change))
138 ≥ 0.4, we obtained the significantly changed unnormalized and normalized phosphoproteins
139 (TGAC8 vs. WT) and imported them into IPA for functional analyses respectively, and
140 compared the canonical pathway enrichments from these two datasets. In IPA, the upstream
141 kinases were predicted based upon the unnormalized phosphoproteom, and the regulatory
142 pathways from the predicted upstream kinases to downstream effective signaling pathways were
143 generated. Molecular and cellular functions were also enriched in IPA. The similar analyses to
144 those conducted in the TGAC8 LV transcriptome were also done in the TGAC8 LV total
145 proteome to observe the GO term enrichment, predicted activities of upstream kinases and
146 phosphatases, and expression of kinases and phosphatases at protein level.

147

148 **6. Analyses of phosphopeptides.**

149 The upregulated phosphopeptides (TGAC8 vs. WT, p-value < 0.05 and log2(fold change) > 0)
150 were processed in R. After split of peptides with multiple phosphosites into individual peptides
151 and filtering of ambiguously identified sites, 2264 phosphopeptides were selected. Protein
152 peptide sequences of full length were downloaded from Uniprot database[12] and matched to the
153 protein accessions corresponding to processed and selected phosphopeptides. Peptides centered
154 on the phosphosites and flanked by 6 amino acids on the N and C termini respectively were
155 extracted from the matched protein peptide sequences, and uploaded into WebLogo[13]
156 (http://weblogo.threeplusone.com/) and iceLogo[14] (https://iomics.ugent.be/icelogoserver/) for
157 sequence motif analysis. In WebLogo online analysis, different amino acids were labeled in
158 different colors representing different chemical properties (refer to figure legend). In iceLogo
159 online analysis, a public amphiphilicity index of polar amino acids reported by Mitaku and
160 colleagues[15] was used as an aid to characterize the amino acid preference at membrane-water
161 interfaces. In addition, the phosphopeptides of PI3K/AKT substates were summarized and
162 displayed in stacked bar plots.

163

164 **7. Integrative analyses of transcriptome, proteome and phosphoproteome.**

165 The changes of significantly regulated molecules (TGAC8 vs. WT, q-value or p-value < 0.05) in
166 transcriptome, total proteome, and unnormalized phosphoproteome were displayed in circos plot.
167 In addition, the changes at different level were compared and visualized in correlation scatter

168 plots. The discordant proteins whose change directions in total proteome and phosphoproteome
169 were opposite were used to analyze the specific regulation at the phosphorylation level by the
170 use of Reactome and GO (Cellular Component and Biological Process) databases.

171 As to the coordinated regulation, the above mentioned significantly regulated molecules
172 (TGAC8 vs. WT) in each dataset were imported into IPA for canonical pathway enrichment.
173 PI3K/AKT signaling and protein ubiquitination were two coordinated pathways across all omics.
174 The phosphopeptides of protein substrates of PI3K were extracted from the phosphopeptide
175 dataset and the numbers of changed phosphopeptides (TGAC8 vs. WT) were summarized and
176 visualized in stacked bar plot. The PI3K/AKT signaling pathway were visualized in IPA, and
177 nodes in the pathways were marked in different colors in terms of their changes at different
178 levels.

179 As kinases and phosphatases are pivotal in phosphorylation, and transcription factors (TFs) are
180 important in transcription regulation, they were extracted from transcriptome, proteome, and
181 phosphoproteome to observe their changes (TGAC8 vs. WT) and deduce their role in the
182 reprogram of phosphoproteome. The upstream transcription regulators including but not only
183 TFs were predicted on the basis of transcriptome and proteome by the utilization of knowledge
184 base in IPA, and their expressions were searched in multiple datasets. Furtherly, TFs that were
185 significantly regulated at phosphorylation level (TGAC8 vs. WT, p-value < 0.05) were defined
186 as significantly changed phosphorylated TFs in this research, and they were uploaded into
187 STRING database[4] (version: 11.0; http://string-db.org/) to generate protein-protein interaction
188 network and enrich KEGG pathways. They were also imported into IPA for canonical pathway,
189 molecular and cellular functions enrichments.

190

191 **8. Western blot.**

192 Snap-frozen left ventricle (LV) tissue from 12-week-old male mice was homogenized and lysed
193 in ice cold RIPA buffer (Thermo Fisher Scientific: 25 mM Tris-HCl (pH 7.6), 150 mM NaCl,
194 1% NP-40, 1% sodium deoxycholate, 0.1% SDS) supplemented with a Halt protease inhibitor
195 cocktail (Thermo Fisher Scientific), Halt phosphatase inhibitor cocktail (Thermo Fisher
196 Scientific) and 1 mM phenylmethyl sulfonyl fluoride, using a Precellys homogenizer (Bertin
197 Instruments) with tissue homogenization kit CKMix (Bertin Instruments) at 4 °C. Extracts were
198 then centrifuged at 10,000×g for 10 min at 4 °C and the protein concentration of the soluble
199 fraction determined using the Bicinchoninic Acid (BCA) Assay (Thermo Fisher Scientific).
200 Samples were denatured in Laemmli sample buffer (BioRad Laboratories) containing 355 mM 2-
201 mercaptoethanol at 95 °C for 5 min, and proteins (10–50 μg/lane) resolved on 4–20% Criterion
202 TGX Stain Free gels (Bio-Rad Laboratories) by SDS/PAGE. Gels then exposed to UV
203 transillumination for 2.5 min to induce crosslinking of Stain Free gel trihalo compound with
204 protein tryptophan residues. Proteins were then transferred to low fluorescence polyvinylidene
205 difluoride (LF-PVDF) membranes (BioRad Laboratories) using an electrophoretic transfer cell

206 (Mini Trans-Blot, Bio-Rad). Membrane total protein was visualized using an Amersham Imager
207 600 (AI600) (GE Healthcare Life Sciences) with UV transillumination to induce and a capture
208 fluorescence signal. Blocked membranes (5% milk/tris-buffered saline with Tween-20, TBST)
209 were incubated with the following primary antibodies: Anti-Phospho-PKA Substrate
210 (RRXS*/T*) antibody, Cell Signaling Technologies, Cat.#9624, 1:1000 dilution; Anti-Phospho-
211 Akt Substrate (RXXS*/T*) antibody, Cell Signaling Technologies, Cat.#9614, 1:1000 dilution;
212 Anti-Ubiquitin antibody produced in rabbit, Sigma-Aldrich, SAB1306582, 1:200 dilution.
213 Primary antibodies were then detected using horseradish peroxidase (HRP) conjugated antibody
214 (Invitrogen) at 1:10,000. Bands were visualized using Pierce SuperSignal West Pico Plus ECL
215 substrate kits (Thermo Scientific), the signal captured using an Amersham Imager 600 (AI600)
216 (GE Healthcare Life Sciences) and quantified using ImageQuant TL software (GE Healthcare
217 Life Sciences). Band density was normalized to total protein.

218

219 **9. Protein synthesis detection.**

220 Protein synthesis was assessed by SUnSET-Western Blot as previously described in the above
221 section. Briefly, the puromycin solution was prepared in PBS, sterilized by filtration, and a
222 volume of 200 µl was injected in mice intraperitoneally, to achieve a final concentration of 0.04
223 µmol/g of body mass. After 30 min, mice were sacrificed, the LV was harvested and snap frozen
224 in liquid nitrogen. Protein extraction was performed using Precellys, quantified with BCA assay
225 25 µg of total protein were separated by SDS-PAGE; proteins were then transferred onto PVDF
226 membrane and incubated overnight in the anti-puromycin primary antibody (MABE343, Sigma-
227 Aldrich, St. Louis, MO). Visualization of puromycin-labeled bands were obtained using
228 horseradish peroxidase conjugated anti-mouse IgG Fc secondary antibody (Jackson
229 ImmunoResearch Laboratories Inc, West Grove, PA, USA), using Pierce Super Signal ECL
230 substrate kit (Pierce/ Thermo Scientific Rockford, IL). Chemiluminescence was captured with
231 the Imager AI600 and densitometry analysis was performed using ImageQuantTL software (both
232 by GE, Boston, MA). Total protein was used as control for protein loading. Genotypic
233 differences of protein synthesis were tested via an as unpaired t-test.

234

235 **10. Proteasome activity detection.**

236 Flash frozen tissue was homogenized in ice-cold cytosolic extraction buffer (50 mM Tris-HCl
237 pH 7.5, 250 mM Sucrose, 5 mM MgCl2, 0.5 mM EDTA, and 1 mM DTT). A bicinchoninic acid
238 (BCA) assay (Pierce) was used to determine the protein concentrations. All samples were equally
239 concentrated in proteasome assay buffer (50 mM Tris-HCl pH 7.5, 40 mM KCl, 5 mM MgCl2,
240 and 1 mM DTT). Proteasome activity was determined in the presence of 28 µM ATP using the
241 Suc-LLVY-AMC (18 µM, Boston Biochem #S280) fluorogenic substrate with and without
242 proteasome inhibition (MG 132, 1 mM, Sigma). The plate was read at an excitation wavelength

243 of 380 nm and an emission wavelength of 469 nm using a Spectramax M5 (Molecular Devices).
244 Activity was calculated by subtracting the background (proteasome inhibited value) from the
245 reading (proteasome activated value).

246

247 **11. Protein soluble and insoluble fractions detection.**

248 Protein aggregates were measured using Proteostat (Enzo, ENZ-51023) following the
249 manufacturer's instructions. For this assay left ventricle myocardial lysate (Cell Signaling lysis
250 buffer) was obtained, protein concentration assayed (BCA assay [Pierce]). Ten µg of protein
251 loaded into a 96-well microplate and protein aggregates were analyzed using the Proteostat assay
252 kit (Enzo Life Sciences) following the manufacturer's instructions. Background readings were
253 subtracted from sample recordings and were normalized to wild-type values.

254

255 **12. Data process and graphics production.**

256 Most raw data were precleared and processed using RStudio (version: 1.1.463) in R language
257 (version: 3.5.3), in which the tidyr package and dplyr package were applied. In addition,
258 GraphPad Prism (version: 7), Microsoft Excel (version: 2019) and Adobe Illustrator (version:
259 CC 2019) were also used for statistics and graphics. Venn diagrams were generated in Venny[5]
260 (version: 2.1.0; http://bioinfogp.cnb.csic.es/tools/venny/index.html). Circos plot was generated
261 using Circos software[6] in Perl language.

262

263

264 **Results**

265 **1. The TGAC8 reprograms the LV phosphoproteome.**

266 The TMT-labeling quantitative MS identified **12963 phospho-peptides** (File 1: Sheet 1) and
267 **3646 phosphoproteins** (File 1: Sheet 2). The principal component analysis (PCA) (Figure 1A)
268 of the 3646 phosphoproteins in each mouse showed that the TG and WT samples were
269 distinguished into two groups completely. The heatmap (Figure 1B) showed the intra-group
270 consistency of upregulated phosphoproteins in TGAC8 compared to WT. Within the cutoff at -
271 log10(p-value) > 1.3 and absolute value of log2(fold-change(TG/WT)) ≥ 0.04, 781
272 phosphoproteins were differentially regulated by genotype. Of the 781 phosphoproteins, the
273 phosphorylation levels of 741 proteins were increased and only 40 were decreased in the TGAC8
274 vs. WT LV (Figure 1C).

275

276 **2. Functional analyses of the phosphoproteome.**

277 We performed the canonical pathway, upstream regulation, and downstream function analyses of
278 the remodeled LV phosphoproteome of TGAC8 using the Ingenuity Pathway Analysis (IPA)
279 software.

280 **2.1. Canonical pathway analysis of the remodeled LV phosphoproteome of TGAC8.**

281 To study the mechanism at phosphorylation level, we first performed canonical pathway analysis
282 using IPA. Top canonical pathways within the phosphoproteome that were statistically
283 differentially enriched in TGAC8 vs. WT were displayed in the bar plot (Figure 1D and File 2:
284 Sheet 1). Of these pathways, cardiac hypertrophy signaling (enhanced) is most highly activated
285 (z-score as high as 4.867) (Figure 1D). The combination of Supplementary Figure 1 and File 2:
286 Sheet 2 and our recently published work[10] showed that the phosphorylation status of numerous
287 molecules, e.g., Ca^{2+} ATPase, RyR2, Ncx, involved in excitation, calcium cycling, contraction,
288 relaxation and protein synthesis, was elevated in the TGAC8 vs. WT LV. However, we have
289 demonstrated that at three-month of age, the mouse age in the present study, the LV mass is not
290 elevated in TGAC8 vs. WT[10]. Of note, transcriptomic, proteomic and WB analyses indicated that
291 pathologic hypertrophic markers were not increased in TGAC8 vs. WT[10]. In this regard, the
292 activation of key stress response signaling pathways, e.g., protein kinase A (PKA) signaling,
293 PI3K signaling, and AMPK signaling, may protect against pathological changes, that result in an
294 increase in cardiac mass in TGAC8 despite its chronic increase in performance. For example,
295 activated PKA signaling can restrict the activity of AC8, acting as a feedback to fine-tune the
296 downstream signaling networks inside the body[3]. Additionally, nitric oxide (NO) signaling may
297 coordinate cardiac protection in the increase in cardiac mass (Figure 1D). Increased
298 phosphorylation status of HSP90 and Akt in TGAC8 synergistically increase eNOS activity[16],
299 and increased NO produced by eNOS may modulate the function of the ryanodine receptor Ca^{2+}
300 release channel (RyR2), which was increased on the PKA dependent phosphopeptides in
301 TGAC8, on the cardiac sarcoplasmic reticulum[17]. The TMT-labeling MS identified significant
302 upregulated phosphorylation in the peptides of RyR2 (RISQTSQVSIDAAHGYSPR, E9Q401
303 [2805-2823]) (File 1: Sheet 1) , consistent with the PKA induced phosphorylation of RyR2-
304 S2809 mediating the increase in Ca^{2+} spark amplitude[18].

305 **2.2. Upstream regulators of the remodeled LV phosphoproteome of TGAC8.**

306 As known, the overexpression of AC8 activates the AC8-cAMP-PKA phosphorylation axis[9].
307 There were 2264 phosphosites whose names and locations are unambiguous within the 4990
308 upregulated phosphopeptides (p-value ≤ 0.05 and log2(fold-change(TG/WT)) ≥ 0) in TGAC8 vs.
309 WT. The majority of these phosphosites were serines (S) and threonines (T), and a few were
310 tyrosines (Y) (Figure 2A). By using WebLogo, we profiled the phosphorylation motif sequences
311 (Figure 2B). A typical PKA and AKT substate motif, R-R-X-pS/T, was the most abundant
312 substrate motif, consistent with increased PKA dependent phosphorylation (Figure 2B-2D)[19,20].
313 In addition to S and T, the center phosphosites also included phosphotyrosine (Y). The center
314 phosphosites were mainly flanked by the P-E-E sequence on the C terminus, endowing a strong

315 hydrophobic and acidic property to the C terminus of the substrate sequences (Figure 2B),
316 supported by the amphiphilicity index analysis in iceLogo (Figure 2E). Because phosphorylation
317 substrate motifs were not restricted to PKA's substrate motif, additional kinases must be also
318 involved in reprogramming the TGAC8 phosphoproteome. Therefore, we were inspired to
319 explore additional kinase-substrate pathways mediating the effect of the cardiac-overexpression
320 of AC8 here.

321 IPA predicted that 26 kinases were responsible for the above-mentioned phosphorylation motifs
322 (File 2: Sheet 3), among which, three had previously been identified to differ by genotype in the
323 LV transcriptome, 18 were shown to differ by genotype in the LV proteome, and 18 were
324 identified in the present phosphoproteome. Of note, most of the identified kinases were
325 upregulated in TGAC8 vs. WT at transcription, translation and PTM (phosphorylation) levels.
326 Within the phosphoproteome, eight kinases were predicted to be differentially activated by
327 genotype, and the phosphorylation level of four of these (PDPK1, PAK1, PTK2B and GSK3B)
328 was increased in TGAC8 vs. WT. These four kinases each phosphorylates various proteins to
329 regulate cellular functions. For example, a previous study observed that in human glioblastoma
330 cell lines, T98G and U87MG cells, the interference of human PDPK1 mRNA by siRNA
331 decreased the phosphorylation level of human BAD protein (S112, S136 and S155) and activated
332 cell death to suppress tumorigenesis[21]. Another study reported that in mouse myoblast cell line,
333 C2C12 cells, PDPK1 protein phosphorylated the mouse ULK1 protein[22]. Increased
334 phosphorylation states of BAD (upregulated at S112, S136 and S155) and ULK1 (upregulated at
335 S450, S521 and S637/638) in TGAC8 may be linked to activated PDPK1.

336 Different kinases can coordinate to reprogram the complex regulation network in the organism.
337 Consistent with the IPA canonical pathway analysis, the phosphorylation level of 27 proteins
338 (including the three kinases (PDPK1, PAK1 and PTK2B) auto-phosphorylating themselves)
339 were elevated by the three kinases to regulate cardiac stress signaling pathways, including PKA
340 signaling, ERK/MAPK signaling, cardiac hypertrophy signaling (enhanced), and renin-
341 angiotensin signaling (Figure 1E), to cope with the cardiac stress in the TGAC8. For example,
342 GSK3B is involved in multiple biological processes. PDPK1 phosphorylated GSK3B at S9[23,24]
343 and PTK2B phosphorylated GSK3B at S9 and Y216[25,26] to inhibit the kinase activity of GSK3B.
344 In this phosphoproteome, GSK3B was phosphorylated at multiple sites, including S9, Y216,
345 S219 and S545, and thus GSK3B inhibition was linked to the cardiac adaptation[27,28].

346 **2.3. Downstream functions of the remodeled LV phosphoproteome of TGAC8.**

347 To study the downstream functions of these phosphoproteins, we performed molecular and
348 cellular functions analysis in IPA. The enriched functions were mainly in three categories, i.e.,
349 cell viability, protein quality control, and metabolism (Figure 1F and File 2: Sheet5). The
350 functions of cellular assembly and organization, cellular function and maintenance, and cell
351 death and survival were ranked as the top three terms, indicating the important role of the

352 reprogrammed phosphoproteome in improving cell viability in response to the chronic stress of
353 the overexpression of AC8 in the mouse heart.

354

355 **3. Integrative analyses of transcriptome, proteome and phosphoproteome.**

356 We next integrated changes in PTM (phosphorylation) in TGAC8 vs. WT with genotypic
357 differences in protein translation and in transcription. The circos plot (Figure 3A) illustrates the
358 genotypic differences (TGAC8 vs. WT) in **molecules** identified across the transcriptome,
359 proteome, and phosphoproteome. In addition, the correlation scatter plots (Figure 3B)
360 demonstrated a moderate level of correlation of genotypic differences of molecular changes
361 within phosphoproteome and transcriptome, and a somewhat stronger correlation between
362 genotypic differences of molecular changes within phosphoproteome and proteome (Figure 3C).
363 Concordant and discordant enrichments of canonical pathways differed by genotype among the
364 three omics are shown in Figure 3D. A comparison of genotypic differences within the three
365 omics highlights the importance of protein phosphorylation, and the phosphorylation was
366 **coordinated with and supplemental to** transcription and translation.

367 Because kinases and phosphatases are the key regulators of phosphorylation, and
368 phosphorylation of transcriptional factors (TFs) are the primary determinant of their activities in
369 transcription, we compared genotypic differences in kinases, phosphatases and TFs within the
370 phosphoproteome and proteome with our previously published genotypic differences in the
371 TGAC8 vs. WT transcriptome[10] (Figure 3E). We identified 196 kinases, 71 phosphatases and
372 191 TFs in the present phosphoproteome (Figure 3F). The protein phosphorylation status of
373 about one half of these molecules differed significantly (p-value < 0.05) by genotype (Figure
374 3G), and the protein phosphorylation status of majority of these molecules was increased (Figure
375 3H-3J). The genotypic differences in the transcription (mRNA expression obtained from RNA-
376 seq) and translation (protein expression obtained from mass spectrometry) of these molecules,
377 however, differed from those in the phosphoproteome (Figure 3E). Because there were more
378 molecules that were unchanged or reduced in the TGAC8 vs. WT transcriptome or proteome
379 than in the phosphoproteome, it is clear that the changes in protein phosphorylation are of utmost
380 importance in the coordination of transcription, translation and PTM, that underlie the adaptive
381 response of the TGAC8 LV to the marked, chronic increase stress of its intrinsically activated
382 AC-cAMP-PKA-Ca^{2+} signaling. Thus, by utilizing multiple bioinformatic analysis methods, we
383 not only dissected the reprogrammed phosphoproteome and deduced its functions in the TGAC8
384 mouse LV, but also profiled the coordination of phosphoproteome, transcriptome and proteome.

385 **3.1. Implications of coordinated changes in protein phosphorylation and transcription in**
386 **TGAC8 vs. WT.**

387 The most likely type of coordination between protein phosphorylation and transcription is related
388 to phosphorylation states of TFs which is determined by kinases and phosphatases activities.

389 Analysis of the remodeled LV transcriptome of TGAC8 in Gene Ontology (GO) analysis using
390 DAVID online software discovered that enrichments of numerous phosphorylation and
391 dephosphorylation related biological processes and molecular functions significantly differed by
392 genotype (Figure 4A), and that the coordinated expression of numerous kinases and
393 phosphatases also differed by genotype (Figure 4B-4C and File 8). Because expression levels of
394 kinases and phosphatases do not denote their activation states, we utilized IPA to predict the
395 genotypic differences in activation states of upstream kinase and phosphatase (regulators of the
396 transcriptome). Intriguingly, 60 kinases were predicted to be upstream regulators of the
397 remodeled LV transcriptome of TGAC8, and the majority of these kinases were predicted to be
398 activated in TGAC8 vs. WT (Figure 4D and File 9). In contrast, many fewer phosphatases were
399 predicted between TGAC8 and WT, and most of these were predicted to be inhibited (Figure 4E
400 and File 9). Thus, the differential genotypic enrichment of phosphorylation status and predicted
401 activation of kinases and phosphatases identified in our post hoc analysis of our previously
402 reported TGAC8 vs. WT transcriptome[10] are linked to the differential genotypic reprogramming
403 of the phosphoproteome discovered in the present study.

404 We utilized IPA to predict the activation states of upstream transcription regulators on the basis
405 of the remodeled LV transcriptomes and proteomes, and then determined their expression levels
406 in transcriptome, proteome and phosphoproteome (Figure 4F). Because TFs are the main
407 regulators of transcription, and because phosphorylation of TFs usually regulates their
408 activities[29-31], we focused our subsequent analysis on functions of those TFs that were
409 differentially phosphorylated in TGAC8 vs. WT. To confirm the hypothesis that the TGAC8
410 might exert transcriptional control by TFs phosphorylation, we retrieved all TFs identified in our
411 previous transcriptome and proteome[10] and mapped them to the current phosphoproteome in
412 order to determine their genotypic differences in phosphorylation status. Of the 191 TFs also
413 identified in this phosphoproteome, 92 TFs differed significantly by genotype in phosphorylation
414 status (p-value < 0.05). In agreement with the general upregulated transcription in TGAC8 LV[10],
415 nearly all of the TFs that differed by genotype had increased phosphorylation level (Figure 4G
416 and File 3). The only exception was purine rich element binding protein G (Purg), known to be
417 hyper-phosphorylated in solid tumors[32].

418 We conducted Kyoto Encyclopedia of Genes and Genomes (KEGG) pathway analysis to further
419 probe the predicted facts of TFs that were generally hyper-phosphorylated in TGAC8 vs. WT.
420 Numerous immunity related pathways, cancer related pathways, and metabolism related
421 pathways were enriched (Figure 4H and File 4). We then utilized IPA for in-depth analysis.
422 Numerous metabolic canonical pathways (glucocorticoid receptor signaling and PPAR
423 signaling), a cancer related canonical pathway (regulation of epithelial-mesenchymal transition
424 pathway), and immunity related canonical pathways (role of JAK1, JAK2 and TYK2 in
425 interferon signaling, IL-9 signaling, JAK/Stat signaling, etc.) were enriched (Figure 4I and File
426 5: Sheet 1). Intriguingly, the sumoylation pathway was markedly inhibited. Because both
427 sumoylation and phosphorylation are important PTMs in transcriptional regulation[33,34], it is

428 possible that the upregulated protein phosphorylation and inhibited protein sumoylation pathway
429 in TFs coordinately activate transcription and improve immunity in the TGAC8 LV. In addition,
430 cell viability and metabolism in molecular and cellular functions were enriched in TGAC8 vs.
431 WT (Figure 4J and File 5: Sheet 2), consistent with enrichments of afore mentioned KEGG
432 pathways and IPA canonical pathways (Figure 4H and 4I).

433 Taken together, we have discovered the existence of substantial crosstalk between protein
434 phosphorylation and transcription in the TGAC8 LV: phosphorylation of TFs reprograms
435 immunity and metabolism pathways and functions in the TGAC8 LV, likely serving to maintain
436 cell survival in response to the chronic stress of marked AC8 overexpression.

437 **3.2. Coordinated changes in protein expression and phosphorylation of the remodeled**
438 **proteome and phosphoproteome of TGAC8.**

439 Having discovered the coordinated changes in the remodeled TGAC8 transcriptome and
440 phosphoproteome (Figure 4A-4E), we next sought to discover the extent to which changes in the
441 remodeled phosphoproteome of the TGAC8 LV were coordinated with changes in its remodeled
442 proteome. Numerous biological processes and molecular functions that were related to
443 phosphorylation and dephosphorylation were enriched in the remodeled TGAC8 LV proteome
444 (Figure 5A), as were numerous kinases and phosphatases (Figure 5B-5C and File 10). Twenty-
445 nine kinases that differed by genotype were predicted to be upstream regulators of the proteome,
446 and most of these were predicted to be activated in TGAC8 vs. WT. Fewer phosphatases than
447 kinases that differed by genotype were identified as upstream regulators of the remodeled
448 TGAC8 LV proteome (Figure 5D-5E and File 11).

449 One strategy adopted to probe deeper into the coordinated changes in the proteome and
450 phosphoproteome of the TGAC8 LV was to normalize the phosphoproteome to the total
451 proteome (in other words, to divide the phosphorylation expression by protein expression) (File
452 1: sheet4). Of the 3927 phosphoproteins identified in our mouse LV samples, 2164 were
453 identified in both the proteome and phosphoproteome, and these were focused for subsequent
454 analyses. After normalization, WT and TGAC8 samples manifested clear genotypic differences
455 in PCA analysis (Figure 5G), and phosphorylation status of numerous proteins normalized to the
456 protein expression level still differed by genotype without cutoff (Figure 5H) and with cutoff (-
457 log(p-value) > 1.3 and absolute(log2(TG/WT)) ≥ 0.4) (Figure 5I). Even after normalizing the
458 phosphorylation level to the protein expression level, the enrichments of canonical pathways in
459 TGAC8 were quite consistent with those of unnormalized phosphoproteome (Figure 5J and File
460 6). Cardiac hypertrophy signaling (enhanced) and cardiac hypertrophy signaling took the top two
461 places, emphasizing the important role of phosphorylation in the regulation of cardiac functions
462 in response to chronic stress when coordinated with changes in the total proteome.

463 Many important stress-response signaling pathways were enriched from phosphoproteome, e.g.,
464 PKA signaling, ERK/MAPK signaling, insulin receptor signaling, and PI3K/AKT signaling
465 (Figure 6A). Three of these pathways, PI3K/AKT, ERK/MAPK and ubiquitin labeling, were also

466 markedly enriched in our previous analysis on total proteome in TGAC8 LV[10]. By integrating
467 and comparing the enrichments from transcriptome, proteome and phosphoproteome, we were
468 able to identify the three signaling pathways in the TGAC8 LV, PI3K/AKT, ERK/MAPK and
469 ubiquitin labeling, that were regulated concordantly in transcription, translation, and PTM
470 (phosphorylation) (Figure 6B). PI3K/AKT and ERK/MAPK signaling pathways are not only
471 enriched but also activated in TGAC8. We verified the phosphorylation and activation of
472 PI3K/AKT (Figure 6E and 7A) and ERK/MAPK (Figure 7B-7C) signaling pathways via WB.
473 Their activations are crucial for the increase in protein synthesis and cell survival in the TGAC8
474 LV[10]. Protein ubiquitination is an important process in protein degradation, which is also
475 increased in TGAC8 LV[10], but the activity of this pathways could not be predicted on the basis
476 of present knowledge base of IPA. Therefore, we conducted wet lab experiments. The rate of
477 protein synthesis was 40% higher in TGAC8 than in WT (Figure 7D). The overall ubiquitination,
478 which labels proteins to be degraded, was increased in TGAC8 vs. WT (Figure 6F), and the
479 proteosome activity, which helps to limit the increased protein load of TGAC8 hearts, was also
480 increased in TGAC8 vs. WT (Figure 7E). Therefore, although there was a significant increase in
481 the amount of soluble misfolded proteins in the TGAC8 LV (Figure 7F), insoluble protein
482 aggregates did not accumulate within the TGAC8 LV (Figure 7G). Our experiment results
483 confirmed the enhanced protein synthesis and degradation to improve the proteostasis.

484 We next sought to identify which molecules linked to PI3K/AKT signaling differed in TGAC8
485 vs. WT. Among the significantly changed upstream molecules, the majority were upregulated.
486 AKT, a central molecule in the pathway, was also increased in proteome and phosphoproteome
487 (Figure 6C). By searching and mapping the substrates of AKT, we unraveled that the
488 phosphorylation levels of AKT peptide substrates were mostly elevated in TGAC8 vs. WT
489 (Figure 6D and Supplementary Figure 3). Therefore, the downstream effects and functions of
490 AKT signaling were activated in TGAC8 LV: (1) upregulating GSK3 to improve energy
491 metabolism; (2) activating mTOR pathway to increase protein synthesis and cell growth; (3)
492 promoting NF-κB mediated transcription; (4) upregulating BAD and eNOS only at
493 phosphorylation level to enhance cell survival and cardiovascular functions. In summary, to
494 adapt the heart to stress for improved survival, the TGAC8 upregulates the protein
495 phosphorylation to reprogram the cardiac LV phosphoproteome.

496

497 **4. Discordant regulation of the phosphoproteome and proteome in TGAC8 LV.**

498 Among the 443 proteins that differed by genotype in both protein phosphorylation and protein
499 expression levels, 33 were changed discordantly at the two levels (in opposite directions, i.e.,
500 upregulated in proteome but downregulated in phosphoproteome, or vice versa) (Figure 8A and
501 File 7: Sheet 1). We uploaded the 33 discordant proteins into STRING online software for
502 functional analyses. The GO_CC (Cellular Component) analysis resulted in many
503 **mitochondrial components**, indicating the involvement of phosphorylated proteins in

504 mitochondria (Figure 8B and File 7: Sheet 2). Reactome pathway analysis showed that in
505 addition to mitochondria, metabolic pathways were enriched significantly in TGAC8 (Figure 8C
506 and File 7: Sheet 3). Mitochondria are the hub of metabolism and multiple metabolic processes
507 are executed in mitochondria. Consistently, both metabolism and mitochondria related processes
508 were ranked the top processes in GO_BP (Biological Process) analysis (Figure 8D and File 7:
509 Sheet 4). Therefore, the discordant part between total proteome and phosphoproteome indicated
510 that the phosphorylation plays a critical role in the regulation of mitochondria and metabolism in
511 the TGAC8, distinct from its role in regulation at the translational level.

512

513 **5. Deduced schematic of coordination of phosphoproteome with transcriptome and**
514 **proteome in TGAC8 mouse LV.**

515 A deduced schematic integration of the remodeled phosphoproteome, proteome and
516 transcriptome of the TGAC8 LV is shown in Figure 9. The TGAC8 mouse first induces a PKA
517 dependent phosphorylation via AC8-cAMP-PKA axis. Many cytoplasmic proteins including TFs
518 are thus phosphorylated and then transported into the nucleus where TFs recognize and bind to
519 the promoters to activate the transcription of more regulatory factors, including kinases,
520 phosphatases, and TFs. The activation states of these factors are changed upon phosphorylated in
521 cytosol, thereby activating additional kinases-controlled phosphorylation cascades and
522 reprogramming the cardiac phosphoproteome comprehensively.

523

524 **Discussion**

525 Our prior study[10] investigated the adaptive mechanisms that emerge in the TGAC8 heart to
526 marked chronic stress of increased AC8-cAMP-PKA-Ca^{2+} signaling. In that study, a large
527 number of proteins differed in TGAC8 vs. WT. The TGAC8 induced a chronic cardiac exercise
528 phenotype in the heart, i.e., an increase in heart rate and contractility. These functional changes
529 were accompanied by an increased cardiac biomass and energy demand. Multiple signaling
530 pathways, related to nutrient sensing, energy production, cardiac cellular stress, cardiac stress
531 response, growth factor signaling, and cell proliferation, were identified as downstream
532 mediating the effect of the activated AC8-cAMP-PKA-Ca^{2+} signaling in the TGAC8 LV.

533 Our goals here were to determine which proteins in TGAC8 LV differed in expression and
534 phosphorylation status compared to WT, and which kinases/phosphatases play a role in these
535 altered phosphorylation statuses in the TGAC8. By the utilization of TMT-labeling MS, we
536 obtained 12963 phosphopeptides and 3646 phosphoproteins, and observed the general
537 upregulation of phosphorylation. We observed the enrichments of phosphorylation, upregulated
538 expression of kinases, and predicted activation of upstream kinases. We made use of
539 phosphoproteome complementary to transcriptome and proteome to expand our understanding of
540 the regulatory mechanism how the TGAC8 adapts to chronic stress of activated AC8-cAMP-

541 PKA-Ca^{2+} signaling. This approach enabled us to appreciate how changes in the transcription,
542 translation and PTM of proteins in the TGAC8 LV may singly or coordinately enable the
543 TGAC8 to endure the chronic AC8-induced stress (Figure 9).

544 First, the TGAC8 induced a PKA dependent phosphorylation via the AC8-cAMP-PKA axis
545 (typical substrate motif of PKA dependent phosphorylation). Most of previous studies only
546 focused on PKA phosphorylated targets as downstream effects of activated AC8. For example,
547 AC8 induced cAMP activates PKA to increase the phosphorylation of many key proteins in
548 cardiovascular system, e.g., ryanodine-receptor-type 2 (RyR2), L-type Ca^{2+} channels (LTCC),
549 phospholamban (PLN or PLB), etc[10]. In this research, we identified 29 phosphosites on RyR2, 15
550 phosphosites on LTCC alpha 1 and beta 2, and 2 phosphosites (S16 and T17) on PLN. SERCA2
551 and the majority of them were increased in phosphorylation statuses in the TGAC8 LV (File 1:
552 Sheet 1). It is worth noting that PLN is phosphorylated on S16 by PKA whereas on T17 by Ca^{2+}-
553 calmodulin-dependent protein kinase (CaMKII)[35].

554 After the activation of phosphorylation cascade, many cytoplasmic proteins including TFs were
555 thus phosphorylated and then transported into the nucleus where TFs recognize and bind to the
556 promoters to activate transcription. For example, Figure 4 F and 4G showed that many
557 transcriptional regulators were phosphorylated in TGAC8 vs. WT. The phosphorylation of
558 STAT1[36,37], STAT3[37], HTT[38] and CREB1[39] is associated with the activation of their
559 transcriptional activities. The elevated TFs phosphorylation and possibly activated transcription
560 were consistent with the general increase in transcriptome[40]. The hyper-phosphorylated TFs
561 might contribute to the improved immunity, metabolism and cell viability in TGAC8 (Figure 4H-
562 4I). For example, STAT family proteins are transcription activators, and their phosphorylation is
563 involved in inflammation and immune response[41,42]. The present study identified increased
564 phosphorylation levels in S727 on STAT1 and S726/S727 on STAT3 (File 1: Sheet 1), in line
565 with our previous report which identified hyper-phosphorylation of components within
566 inflammation and immune response signaling pathways such as JAK/STAT and JNK
567 pathways[10].

568 Upon the activation of RNA transcription, numerous molecules, including kinases, phosphatases,
569 and TFs, were transcribed more in TGAC8 than WT, thereby, activating other kinases-controlled
570 phosphorylation cascades in addition to PKA. The additional kinases and phosphorylation
571 cascades could also be directly activated by the overexpression of AC8 in another manner to be
572 determined. In this study, with the three datasets, IPA predicted many other kinase-substrate
573 reactions in addition to PKA. PDPK1, PAK1 and PTK2B were the three most consistent kinases.
574 In the context of the overexpression of AC8, these three kinases could be activated to
575 phosphorylate multiple proteins to activate PKA pathway (positive feedback) and MAPK/ERK
576 pathway (also known as Ras-Raf-MEK-ERK pathway) to maintain heart health (Figure 1E and
577 Supplementary Figure 2). Previously, we showed their western blot results that MAPK/ERK
578 pathway were activated due to increased protein expression of p21 Ras and the elevated
579 phosphorylation levels of c-Raf, MEK1/2 and ERK1/2 as well as their increased ratios of

580 phosphorylation to protein expression[10]. In the present study, S233 and S621/S641 on Isoform 2
581 of RAF proto-oncogene serine/threonine-protein kinase were hyper-phosphorylated in TGAC8
582 (File 1: Sheet 1). Importantly, the multifunctional molecule, GSK3B, was the downstream of
583 PDPK1 and PTK2B in the integrated regulation network. GSK3B is involved in metabolism and
584 cardiac hypertrophy[43,44]. Interestingly, AC8 is required for glucose homeostasis and
585 hypothalamic adaptation to high-fat diet[45]. The phosphorylation of GSK3B is also a critical
586 mediator in convergence of cardioprotection signaling[27,28]. We previously detected the increase
587 in the protein expression of GSK3B[10] and here identified the hyper-phosphorylated S9 on
588 GSK3B (File 1: Sheet 1). The bioinformatic analysis strategy here revealed a larger kinase-
589 substrate network important in the remodeling of the TGAC8 heart. We plan to validate these
590 kinase-substrate reactions in follow-up studies and provide the reliable mechanism in
591 cardiovascular research.

592 Taken together, the TGAC8 upregulates phosphorylation to reprogram the heart. Based on
593 results in this study combined with our recently published work on TGAC8 LV[10], we generated a
594 comprehensive circuitry (Figure 10). Navigating this figure "by the numbers": marked, chronic,
595 cardiac specific overexpression of AC8 (1) chronically increases cAMP (2) and PKA-Ca^{2+}
596 signaling (3), resulting, not only in an incessantly increased cardiac performance, due to elevated
597 heart rate and LV contractility (4), but also activation of growth factor signaling pathways (5),
598 leading to increase in energy demand due to increased transcription and increased amino acid,
599 nucleotide, protein, lipid and lipoprotein synthesis, increased protein quality control, including
600 proteosome activity, autophagy, mitophagy, cytokine signaling and inflammation (6). Chronic
601 high level of AC8 activation elicits numerous stress responses (8) including increased nutrient
602 sensing with increased AMPK signaling (10A), increased ROS scavenging, protection against
603 cell death, and also induction of signaling to minimize the impact of AC-PKA signaling (10B).
604 Shifts in energy production and utilization to deal with the marked energy demands of the
605 TGAC8 heart (10, 12) include: enhancement of glucose metabolism is pronounced (11, 13),
606 whilst utilization of fatty acids to produce energy is reduced (11) but an increase in glucose
607 catabolism (10, 11) is accompanied by an increased anabolism (12), supported by increased
608 aerobic glycolysis (11,13); increased utilization of the pentose phosphate shunt (5, 13) supports
609 increased amino acid, nucleotide, protein and lipoprotein synthesis induced by growth factor
610 signaling (5), resulting in an increase in LV biomass (14). This adaptive profile balances energy
611 requirements necessary for an incessant marked increase in cardiac performance (4), for
612 increased RNA transcription, protein translation and quality control required for cardiac growth
613 (14), and for other biological processes within the LV myocardium (6). This pattern of consilient
614 adaptations (6-15) sustains an incessant increase in cardiac performance while conferring cardio-
615 protection to the TGAC8 heart.

616 In addition to the fascinating adaptive mechanisms in the TGAC8 LV discussed above, the
617 present research also raised some interesting open-mind questions, such as cardiac hypertrophy
618 signaling and sumoylation pathway enriched here.

619 Although the cardiac β-AR signaling is desensitized in many pathological conditions, like aging,
620 so as to despair the cardiovascular system functions, cAMP bioavailability could maintain
621 cardiac functions in the aged heart. Based on this, the overexpression of AC8 in heart was
622 regarded as a potential therapeutic way to increase the bioavailability of cardiac cAMP
623 independent of β-AR stimulation to improve cardiac functions[7]. Unexpectedly, the cardiac-
624 specific chronic activation of the cAMP pathway (overexpressing β1- AR, β2-AR, Gas, PKA,
625 PP1 inhibitor-1 (I-1), etc.) that enhances cardiac functions in young animals induces progressive
626 cardiomyopathy and premature death during aging[46]. Consistently, in the present research,
627 although the enriched cardiac hypertrophy signaling (enhanced) was not accompanied with the
628 markable hypertrophy phenotype in young male TGAC8 mice, it indicated a cardiac remodeling
629 that could lead to hypertrophy if accompanied with additional stresses, like aging. This
630 assumption was supported by another research on the TGAC8 mouse which reported early
631 alterations of myocardial structure, i.e., cardiomyocyte hypertrophy and endocardial fibrosis, in
632 twelve-month old TGAC8 mice compared with their WT littermates[47]. Therefore, our established
633 bioinformatic analysis strategy is a novel paradigm in **predicting** progressive cardiomyopathy
634 and premature death using early reprograming of omics in young age. More importantly, the
635 mechanisms discovered here in the young adult TGAC8 mice could be utilized in maintaining
636 cardiac health in older TGAC8 mice.

637 Interestingly, more and more PTMs have been discovered nowadays and they often occur at the
638 same time or on the same protein to carry important biological processes coordinately[48,49]. For
639 example, in rat hearts subjected to ischemia, lysine acetylation interferes with activities of
640 protein kinases to increase proximal dephosphorylation, which is involved in the regulation of
641 cell survival or death[50]. In the present research, sumoylation pathway was inhibited along with
642 the upregulated phosphorylation (Figure 4I), indicating the cross-talk between these two PTMs
643 in the mouse heart. In human cell-lines, the switch from phosphorylation to sumoylation could
644 repress the Raf/MEK/ERK signaling to improve the immunity, resulting in the declined infection
645 of influenza A virus[51]. In human HEK293 cells, the coordinated phosphorylation and
646 sumoylation can also control MEF2 transcriptional activity[52]. However, the competition of
647 phosphorylation and sumoylation in cardiomyocytes was unclear. In this research, we observed
648 the upregulated phosphorylation and inhibited sumoylation pathway enriched from TFs in the
649 TGAC8 mouse LV. The regulated PTMs were speculated to be involved in the increased
650 transcription and improved immunity. To validate the effect on sumoylation by elevated
651 phosphorylation in our next studies, we could perform WB with the antibody against pan-
652 sumoylation to detect the general sumoylation change in the TGAC8 LV. In addition, we could
653 detect the sumoylation changes after mimicry upregulation or downregulation of phosphorylation
654 using activators or inhibitors in primary cardiomyocytes to prove the interplay between
655 phosphorylation and sumoylation in cardiomyocytes.

656 In summary, the reprogrammed phosphoproteome activated stress response signaling pathways
657 to defend against cardiac stress in young mice, improve cell viability and suppress cell death. On

658 one hand, the reprogramed phosphoproteome enhances transcription to improve the immunity
659 and metabolism; on the other hand, it coordinates with the proteome to improve mitochondrial
660 functions and metabolism. Finally, although we revealed the coordination of regulation at
661 different levels, which provides a roadmap to guide the integration of transcription, translation
662 and PTM, our results set the stage for additional studies in this remarkable TGAC8 model: What
663 kinases are specifically involved in the PTM identified here? How are these phosphorylated
664 proteins specifically distributed in subcellular locations? The present study focuses on a
665 comprehensive in silico analysis of functionally coherent and data-driven transcription,
666 translation, and post-translation patterns that were well translated in the contribution to AC8-
667 overexpression cardiac outcomes, while further investigation is warranted to see whether the hub
668 pathway/function predictions via gene sets, phosphopeptides, and phosphoproteins could be used
669 as biomarkers or impact the diagnostic specificity for transgenic AC8 cardiac health and
670 pathology.

671

672 **Acknowledgements**

673 We thank all members in Laboratory of Cardiovascular Science, National Institute on Aging, National
674 Institutes of Health, for technical assistance and discussion. This work utilized the computational
675 resources of the NIH HPC Biowulf cluster (http://hpc.nih.gov).

676

677 **Sources of Funding**

678 Intramural Research Program at National Institute on Aging, National Institutes of Health.

679

680 **Disclosures**

681 None.

682

683 **References**

684 1 Halls, M. L. & Cooper, D. M. F. Adenylyl cyclase signalling complexes - Pharmacological
685 challenges and opportunities. *Pharmacol Ther* **172**, 171-180 (2017).
686 https://doi.org:10.1016/j.pharmthera.2017.01.001
687 2 Dessauer, C. W. *et al.* International Union of Basic and Clinical Pharmacology. CI. Structures and
688 Small Molecule Modulators of Mammalian Adenylyl Cyclases. *Pharmacological reviews* **69**, 93-
689 139 (2017). https://doi.org:10.1124/pr.116.013078
690 3 Willoughby, D. *et al.* A key phosphorylation site in AC8 mediates regulation of Ca(2+)-dependent
691 cAMP dynamics by an AC8-AKAP79-PKA signalling complex. *J Cell Sci* **125**, 5850-5859 (2012).
692 https://doi.org:10.1242/jcs.111427

693 4 Sadana, R. & Dessauer, C. W. Physiological roles for G protein-regulated adenylyl cyclase
694 isoforms: insights from knockout and overexpression studies. *Neuro-Signals* **17**, 5-22 (2009).
695 https://doi.org:10.1159/000166277
696 5 Georget, M. *et al.* Augmentation of cardiac contractility with no change in L-type Ca2+ current in
697 transgenic mice with a cardiac-directed expression of the human adenylyl cyclase type 8 (AC8).
698 *Faseb j* **16**, 1636-1638 (2002). https://doi.org:10.1096/fj.02-0292fje
699 6 Ferguson, G. D. & Storm, D. R. Why calcium-stimulated adenylyl cyclases? *Physiology (Bethesda,*
700 *Md.)* **19**, 271-276 (2004). https://doi.org:10.1152/physiol.00010.2004
701 7 Lipskaia, L. *et al.* Enhanced cardiac function in transgenic mice expressing a Ca(2+)-stimulated
702 adenylyl cyclase. *Circ. Res.* **86**, 795-801 (2000). https://doi.org:10.1161/01.res.86.7.795
703 8 Esposito, G. *et al.* Increased myocardial contractility and enhanced exercise function in
704 transgenic mice overexpressing either adenylyl cyclase 5 or 8. *Basic Res Cardiol* **103**, 22-30
705 (2008). https://doi.org:10.1007/s00395-007-0688-6
706 9 Moen, J. M. *et al.* Overexpression of a Neuronal Type Adenylyl Cyclase (Type 8) in Sinoatrial
707 Node Markedly Impacts Heart Rate and Rhythm. *Front Neurosci* **13**, 615 (2019).
708 https://doi.org:10.3389/fnins.2019.00615
709 10 Tarasov, K. V. *et al.* A remarkable adaptive paradigm of heart performance and protection
710 emerges in response to the constitutive challenge of marked cardiac-specific overexpression of
711 adenylyl cyclase type 8. *eLife* **11**, e80949 (2022). https://doi.org:10.7554/eLife.80949
712 11 Qu, J.-H. *et al.* Proteomic Landscape and Deduced Functions of the Cardiac 14-3-3 Protein
713 Interactome. *Cells* **11**, 3496 (2022). https://doi.org:10.3390/cells11213496
714 12 Consortium, T. U. UniProt: a worldwide hub of protein knowledge. *Nucleic Acids Res.* **47**, D506-
715 D515 (2018). https://doi.org:10.1093/nar/gky1049
716 13 Crooks, G. E., Hon, G., Chandonia, J. M. & Brenner, S. E. WebLogo: a sequence logo generator.
717 *Genome research* **14**, 1188-1190 (2004). https://doi.org:10.1101/gr.849004
718 14 Colaert, N., Helsens, K., Martens, L., Vandekerckhove, J. & Gevaert, K. Improved visualization of
719 protein consensus sequences by iceLogo. *Nat Methods* **6**, 786-787 (2009).
720 https://doi.org:10.1038/nmeth1109-786
721 15 Mitaku, S., Hirokawa, T. & Tsuji, T. Amphiphilicity index of polar amino acids as an aid in the
722 characterization of amino acid preference at membrane-water interfaces. *Bioinformatics* **18**,
723 608-616 (2002). https://doi.org:10.1093/bioinformatics/18.4.608
724 16 Takahashi, S. & Mendelsohn, M. E. Synergistic activation of endothelial nitric-oxide synthase
725 (eNOS) by HSP90 and Akt: calcium-independent eNOS activation involves formation of an
726 HSP90-Akt-CaM-bound eNOS complex. *The Journal of biological chemistry* **278**, 30821-30827
727 (2003). https://doi.org:10.1074/jbc.M304471200
728 17 Lim, G., Venetucci, L., Eisner, D. A. & Casadei, B. Does nitric oxide modulate cardiac ryanodine
729 receptor function? Implications for excitation-contraction coupling. *Cardiovasc Res* **77**, 256-264
730 (2008). https://doi.org:10.1093/cvr/cvm012
731 18 Meissner, G. in *Structure and Function of Calcium Release Channels Current Topics in*
732 *Membranes* 91-113 (2010).
733 19 Hunzicker-Dunn, M. E. *et al.* PKA and GAB2 play central roles in the FSH signaling pathway to
734 PI3K and AKT in ovarian granulosa cells. *Proceedings of the National Academy of Sciences of the*
735 *United States of America* **109**, E2979-2988 (2012). https://doi.org:10.1073/pnas.1205661109
736 20 Bellis, A. *et al.* Cross-talk between PKA and Akt protects endothelial cells from apoptosis in the
737 late ischemic preconditioning. *Arterioscler Thromb Vasc Biol* **29**, 1207-1212 (2009).
738 https://doi.org:10.1161/atvbaha.109.184135

739 21 Desai, S., Pillai, P., Win-Piazza, H. & Acevedo-Duncan, M. PKC-iota promotes glioblastoma cell
740 survival by phosphorylating and inhibiting BAD through a phosphatidylinositol 3-kinase pathway.
741 *Biochim Biophys Acta* **1813**, 1190-1197 (2011). https://doi.org:10.1016/j.bbamcr.2011.03.007
742 22 Li, Y. *et al.* microRNA-378 promotes autophagy and inhibits apoptosis in skeletal muscle.
743 *Proceedings of the National Academy of Sciences of the United States of America* **115**, E10849-
744 e10858 (2018). https://doi.org:10.1073/pnas.1803377115
745 23 Chen, X. *et al.* PDK1 regulates platelet activation and arterial thrombosis. *Blood* **121**, 3718-3726
746 (2013). https://doi.org:10.1182/blood-2012-10-461897
747 24 Ericson, K. *et al.* Genetic inactivation of AKT1, AKT2, and PDPK1 in human colorectal cancer cells
748 clarifies their roles in tumor growth regulation. *Proceedings of the National Academy of Sciences*
749 *of the United States of America* **107**, 2598-2603 (2010).
750 https://doi.org:10.1073/pnas.0914018107
751 25 Hartigan, J. A., Xiong, W. C. & Johnson, G. V. Glycogen synthase kinase 3beta is tyrosine
752 phosphorylated by PYK2. *Biochemical and biophysical research communications* **284**, 485-489
753 (2001). https://doi.org:10.1006/bbrc.2001.4986
754 26 Tsai, C. C. *et al.* Glycogen synthase kinase-3beta facilitates IFN-gamma-induced STAT1 activation
755 by regulating Src homology-2 domain-containing phosphatase 2. *J Immunol* **183**, 856-864 (2009).
756 https://doi.org:10.4049/jimmunol.0804033
757 27 Juhaszova, M. *et al.* Glycogen synthase kinase-3beta mediates convergence of protection
758 signaling to inhibit the mitochondrial permeability transition pore. *The Journal of clinical*
759 *investigation* **113**, 1535-1549 (2004). https://doi.org:10.1172/JCI19906
760 28 Juhaszova, M. *et al.* Role of glycogen synthase kinase-3beta in cardioprotection. *Circ. Res.* **104**,
761 1240-1252 (2009). https://doi.org:10.1161/CIRCRESAHA.109.197996
762 29 Bohmann, D. Transcription factor phosphorylation: a link between signal transduction and the
763 regulation of gene expression. *Cancer cells (Cold Spring Harbor, N.Y. : 1989)* **2**, 337-344 (1990).
764 30 Weigel, N. L. & Moore, N. L. Steroid receptor phosphorylation: a key modulator of multiple
765 receptor functions. *Molecular endocrinology (Baltimore, Md.)* **21**, 2311-2319 (2007).
766 https://doi.org:10.1210/me.2007-0101
767 31 Mayr, B. & Montminy, M. Transcriptional regulation by the phosphorylation-dependent factor
768 CREB. *Nature reviews. Molecular cell biology* **2**, 599-609 (2001).
769 https://doi.org:10.1038/35085068
770 32 Zanivan, S. *et al.* Solid tumor proteome and phosphoproteome analysis by high resolution mass
771 spectrometry. *J Proteome Res* **7**, 5314-5326 (2008). https://doi.org:10.1021/pr800599n
772 33 Tomanov, K. *et al.* Sumoylation and phosphorylation: hidden and overt links. *Journal of*
773 *Experimental Botany* **69**, 4583-4590 (2018). https://doi.org:10.1093/jxb/ery167
774 34 Khan, M. *et al.* Interplay between phosphorylation and SUMOylation events determines CESTA
775 protein fate in brassinosteroid signalling. *Nat Commun* **5**, 4687 (2014).
776 https://doi.org:10.1038/ncomms5687
777 35 Wegener, A. D., Simmerman, H. K., Lindemann, J. P. & Jones, L. R. Phospholamban
778 phosphorylation in intact ventricles. Phosphorylation of serine 16 and threonine 17 in response
779 to beta-adrenergic stimulation. *The Journal of biological chemistry* **264**, 11468-11474 (1989).
780 36 Pilz, A. *et al.* Phosphorylation of the Stat1 transactivating domain is required for the response to
781 type I interferons. *EMBO reports* **4**, 368-373 (2003). https://doi.org:10.1038/sj.embor.embor802
782 37 Wen, Z., Zhong, Z. & Darnell, J. E., Jr. Maximal activation of transcription by Stat1 and Stat3
783 requires both tyrosine and serine phosphorylation. *Cell* **82**, 241-250 (1995).
784 https://doi.org:10.1016/0092-8674(95)90311-9

785 38 Kumar, A., Vaish, M. & Ratan, R. R. Transcriptional dysregulation in Huntington's disease: a
786 failure of adaptive transcriptional homeostasis. *Drug Discov. Today* **19**, 956-962 (2014).
787 https://doi.org:10.1016/j.drudis.2014.03.016
788 39 Wang, H., Xu, J., Lazarovici, P., Quirion, R. & Zheng, W. cAMP Response Element-Binding Protein
789 (CREB): A Possible Signaling Molecule Link in the Pathophysiology of Schizophrenia. *Frontiers in*
790 *molecular neuroscience* **11**, 255-255 (2018). https://doi.org:10.3389/fnmol.2018.00255
791 40 Tarasov, K. V. *et al.* A Remarkable Adaptive Paradigm Of Heart Performance And Protection
792 Emerges In Response To The Constitutive Challenge of Marked Cardiac-Specific Overexpression
793 Of Adenylyl Cyclase Type 8. *bioRxiv*, 2022.2005.2020.491883 (2022).
794 https://doi.org:10.1101/2022.05.20.491883
795 41 Seif, F. *et al.* The role of JAK-STAT signaling pathway and its regulators in the fate of T helper
796 cells. *Cell Communication and Signaling* **15**, 23 (2017). https://doi.org:10.1186/s12964-017-
797 0177-y
798 42 Decker, T. & Kovarik, P. Serine phosphorylation of STATs. *Oncogene* **19**, 2628-2637 (2000).
799 https://doi.org:10.1038/sj.onc.1203481
800 43 Beurel, E., Grieco, S. F. & Jope, R. S. Glycogen synthase kinase-3 (GSK3): regulation, actions, and
801 diseases. *Pharmacol Ther* **148**, 114-131 (2015).
802 https://doi.org:10.1016/j.pharmthera.2014.11.016
803 44 Lal, H., Ahmad, F., Woodgett, J. & Force, T. The GSK-3 family as therapeutic target for myocardial
804 diseases. *Circ Res* **116**, 138-149 (2015). https://doi.org:10.1161/circresaha.116.303613
805 45 Raoux, M. *et al.* Multilevel control of glucose homeostasis by adenylyl cyclase 8. *Diabetologia*
806 **58**, 749-757 (2015). https://doi.org:10.1007/s00125-014-3445-z
807 46 El-Armouche, A. & Eschenhagen, T. Beta-adrenergic stimulation and myocardial function in the
808 failing heart. *Heart failure reviews* **14**, 225-241 (2009). https://doi.org:10.1007/s10741-008-
809 9132-8
810 47 Mougenot, N. *et al.* Cardiac adenylyl cyclase overexpression precipitates and aggravates age-
811 related myocardial dysfunction. *Cardiovascular research* **115**, 1778-1790 (2019).
812 https://doi.org:10.1093/cvr/cvy306
813 48 Beltrao, P., Bork, P., Krogan, N. J. & van Noort, V. Evolution and functional cross-talk of protein
814 post-translational modifications. *Molecular systems biology* **9**, 714 (2013).
815 https://doi.org:10.1002/msb.201304521
816 49 Venne, A. S., Kollipara, L. & Zahedi, R. P. The next level of complexity: crosstalk of
817 posttranslational modifications. *Proteomics* **14**, 513-524 (2014).
818 https://doi.org:10.1002/pmic.201300344
819 50 Parker, B. L. *et al.* Structural basis for phosphorylation and lysine acetylation cross-talk in a
820 kinase motif associated with myocardial ischemia and cardioprotection. *The Journal of biological*
821 *chemistry* **289**, 25890-25906 (2014). https://doi.org:10.1074/jbc.M114.556035
822 51 Wang, C. *et al.* HA Triggers the Switch from MEK1 SUMOylation to Phosphorylation of the ERK
823 Pathway in Influenza A Virus-Infected Cells and Facilitates Its Infection. *Frontiers in cellular and*
824 *infection microbiology* **7**, 27 (2017). https://doi.org:10.3389/fcimb.2017.00027
825 52 Grégoire, S. *et al.* Control of MEF2 transcriptional activity by coordinated phosphorylation and
826 sumoylation. *The Journal of biological chemistry* **281**, 4423-4433 (2006).
827 https://doi.org:10.1074/jbc.M509471200

828

829

830 **Figure Legends**

831 **Figure 1. TGAC8 reprograms the LV phosphorylation state. A**. PCA plot of phosphoproteome in
832 TGAC8 vs. WT LVs. **B**. Heatmap of scaled expressions of phosphorylated proteins. **C**. Volcano plot of
833 phosphoproteome. Red dots represent upregulated phosphoproteins with -log10(p-value) > 1.3 and
834 log2(fold change) ≥ 0.4; blue dots represent downregulated phosphoproteins with -log10(p-value) > 1.3
835 and log2(fold change) ≤ -0.4; grey dots represent nonsignificantly regulated phosphoproteins with -
836 log10(p-value) ≤ 1.3 or absolute(log2(fold change)) < 0.4. **D**. Top 21 canonical pathways enriched from
837 phosphoproteome. Orange and blue bars represent activated and inhibited pathways respectively. The
838 darker the color is, the greater the absolute(z-score) is, and the more significantly enriched the pathway is.
839 **E**. Regulatory pathway from upstream kinases. Three dots in the center represent the predicted upstream
840 kinases. Surrounding dots represent identified phosphoproteins differentially regulated in
841 phosphoproteome. Terms on the bottom represent canonical pathways in which the phosphoproteins are
842 involved. Meanings of colors refer to the box of prediction legend besides the graph. **F**. Enriched
843 molecular and cellular functions from the phosphoproteome. They are related to three categories,
844 including cell viability, protein quality control, and metabolism.

845

846 **Figure 2. Characteristics of upregulated phosphopeptides. A**. Composition of phosphosites that reside
847 on the upregulated phosphopeptides. **B**. Sequence logo diagrams of upregulated phosphopeptides centered
848 on the phosphosites and flanked by 6 amino acids on the N and C termini respectively using WebLogo
849 online software. Colors of amino acids represent different chemical properties. **C**. Test the amphiphilicity
850 feature of the upregulated phosphopeptides using iceLogo online software and referring to a published
851 work by Mitaku and colleagues in 2002. **D-E**. Western blots of phosphorylation of PKA substrates and
852 their statistics results: RRXS*/T* (D) and RXXS*/T* (E). Unpaired t test with Welch's correction was
853 used.

854

855 **Figure 3. Integrative analysis of transcriptome, proteome and phosphoproteome. A**. Circos plot of
856 gene expression at different levels from transcription, to protein, and to phosphorylation. Bars in each
857 layer of circle represent changes of significantly regulated molecules (q-value or p-value < 0.05) in
858 transcriptome, total proteome, and unnormalized phosphoproteome. Bar height, color and direction
859 represent log2(fold change). Red and upward indicate upregulation, and blue and downward indicate
860 downregulation. **B-C**. Scatter plots of correlation between phosphoproteome and transcriptome (**B**) or
861 total proteome (**C**). **D**. Comparison of canonical pathway enrichments from the transcriptome, total
862 proteome, and phosphoproteome. Enrichment z-scores were calculated in IPA, and were scaled to
863 generate heatmap in R language. **E**. Integrative graph of expression of all phosphoproteins and selected
864 types of molecules. Bar plot on the bottom displays expression of all significantly changed (p-value <
865 0.05) phosphoproteins in unnormalized phosphoproteome. Y-axis denotes log2(fold change), and x-axis
866 denotes each molecule ranked by log2(fold change). Bars were colored by -log10(p-value). Stick plots on
867 the top display kinases, phosphatases and transcription factors (TFs) selected from the bottom bar plot and
868 their changes in transcriptome (RNA), total proteome (pro), and normalized phosphoproteome (norm).
869 From top to bottom: each large block denotes the changes of certain types of molecules (from kinases to
870 phosphatases, to TFs). In each block, the three rows from top to bottom indicate the changes in
871 transcriptome, total proteome, and normalized phosphoproteome. Each stick represents a molecule and
872 color represents the change: red: (p-value or q-value < 0.05) and log2FC > 0; blue: (p-value or q-value <

873 0.05) and log2FC < 0; black: (p-value or q-value ≥ 0.05) or log2FC = 0; grey: unidentified in one of the
874 omics. Their locations are matched to those in the bottom bar plot. **F-J**. Pie plots of composition of
875 phosphoproteins in the unnormalized phosphoproteome. Regardless of p-value, numbers of four types of
876 proteins, including kinases, phosphatases, TFs and others, are displayed in **F**. After filtration with cutoff
877 p-value < 0.05, numbers of those types of proteins are displayed in **G**. Extracted from G, numbers of
878 upregulated and downregulated kinases (**H**), phosphatases (**I**) and TFs (**J**) are displayed.

879

880 **Figure 4. Coordination of phosphoproteome and transcriptome. A**. GO term enrichments of
881 biological processes and molecular functions about phosphorylation and dephosphorylation from
882 transcriptome. **B-C**. Changes of kinases (**B**) and phosphatases (**C**) whose q-values are less than 0.05 in
883 transcriptome. **D-E**. States of upstream kinases (**D**) and phosphatases (**E**) predicted based on
884 transcriptome. Z-scores were calculated in IPA. Positive and negative z-scores indicate activated and
885 inhibited states respectively. The larger absolute values of z-score indicate more activated or inhibited
886 states. **F**. Heatmap of predicted upstream transcription regulators (left) and their changes in different
887 omics datasets (right). Left: Fill color represent activation z-scores in transcriptome and total proteome.
888 Red and blue indicate activated and inhibited states respectively. Molecules are ranked by z-scores in
889 transcriptome. Right: Fill color represent changes in transcriptome, total proteome, unnormalized
890 phosphoproteome, and normalized phosphoproteome: orange: (p-value or q-value < 0.05) and log2FC >
891 0; yellow: (p-value or q-value ⩾ 0.05) and log2FC > 0; green: (p-value or q-value < 0.05) and log2FC <
892 0; light blue: (p-value or q-value ⩾ 0.05) and log2FC < 0; grey: unidentified in one of the omics. **G**.
893 Changes of differentially regulated TFs with p-value < 0.05 in the unnormalized phosphoproteome. **H**.
894 KEGG pathway enrichments of the differentially regulated TFs. They are in four primary categories:
895 cancer, immunity, metabolism and others. **I**. Top 20 canonical pathways enriched from the
896 phosphoproteome using IPA. The darker the color is, the greater the absolute(z-score) is, and the more
897 significantly enriched the pathway is. **J**. Enriched molecular and cellular functions from the
898 phosphoproteome using IPA. They are in two primary categories: cell viability and metabolism.

899

900 **Figure 5. Analysis of normalized phosphoproteome. A**. GO term enrichments of biological processes
901 and molecular functions about phosphorylation and dephosphorylation from the present proteome. **B-C**.
902 Changes of kinases (**B**) and phosphatases (**C**) whose q-values are less than 0.05 in previous proteome. **D-**
903 **E**. States of upstream kinases (**D**) and phosphatases (**E**) predicted based on the present proteome. Z-scores
904 were calculated in IPA. Positive and negative z-scores indicate activated and inhibited states respectively.
905 The larger absolute values of z-score indicate more activated or inhibited states. **F**. Venn plot of new total
906 proteome and unnormalized phosphoproteome that were conducted concurrently in the same platform. **G**.
907 PCA plot of phosphoproteome normalized to total proteome. **H**. Heatmap of expressions of
908 phosphoproteins normalized to total proteins. **I**. Volcano plot of normalized phosphoproteome. Red dots
909 represent upregulated phosphoproteins with -log10(p-value) > 1.3 and log2(fold change) ⩾ 0.4; blue dots
910 represent downregulated phosphoproteins with -log10(p-value) > 1.3 and log2(fold change) ⩽ -0.4; grey
911 dots represent nonsignificantly regulated phosphoproteins with -log10(p-value) ⩽ 1.3 or
912 absolute(log2(fold change)) < 0.4. **J**. Comparison of canonical pathway enrichments between
913 unnormalized and normalized phosphoproteome. Orange fill colors indicate that all comparable pathways

914 on the top are activated in both omics datasets. The darker the color is, the greater the absolute(z-score) is,
915 and the more significantly enriched the pathway is.

916

917 **Figure 6. Coordinated regulation of transcriptome, proteome and phosphoproteome on PI3K/AKT**
918 **and ERK/MAPK signaling pathways and protein synthesis and degradation. A**. Canonical pathway
919 enrichment of phosphoproteome only with cutoff p-value < 0.05. The darker the color is, the greater the
920 absolute(z-score) is, and the more significantly enriched the pathway is. **B**. Comparison of PI3K/AKT
921 signaling and protein ubiquitination pathways enriched from transcriptome (red outline), proteome (blue
922 outline) and phosphoproteome (green outline). **C**. Pathway graph of PI3K/AKT signaling marked with
923 changes in transcriptome (left box), proteome (middle box) and phosphoproteome (right box). Fill colors
924 indicate changes: red and green indicate upregulation and downregulation respectively; grey indicates
925 nonsignificant regulation. **D**. Phosphopeptide number of substrates of PI3K. Y-axis represents protein
926 substates of PI3K; x-axis represents number of phosphopeptides. Red and blue bars indicate upregulated
927 (p-value < 0.05 and log2(fold change) > 0) and downregulated (p-value < 0.05 and log2(fold change) < 0)
928 phosphopeptides respectively. **E**. Western blot verification of phosphorylation and activation of
929 PI3K/AKT signaling pathway in TGAC8 vs. WT. **F**. Western blot of ubiquitination in TGAC8 vs. WT.

930

931 **Figure 7. Cross verification of activated PI3K/AKT and ERK/MAPK signaling pathways and**
932 **enhanced protein synthesis and degradation from our previous study. A.** Western blot verification of
933 phosphorylation and activation of PI3K/AKT signaling pathway in TGAC8 vs. WT. **B-C.** Western blot
934 verification of phosphorylation and activation of ERK/MAPK signaling pathway in TGAC8 vs. WT. **D.**
935 Confirmation of enhanced protein synthesis in TGAC8 vs. WT. **E.** The enhanced proteasome activity in
936 TGAC8 vs. WT. **F-G.** The soluble misfolded proteins were increased in TGAC8 LV (**F**) whereas the
937 insoluble protein aggregates did not accumulate within the TGAC8 vs. WT (**G**). These panels were
938 adapted from figures in our recently published and closely associated work[10] whose experiments were
939 repeated and results were reproduced in this study.

940

941 **Figure 8. Analyses of proteins changed discordantly in proteome and phosphoproteome. A**. Venn
942 diagram of significantly regulated proteins in total proteome and significantly regulated phosphoproteins
943 in unnormalized phosphoproteome that were conducted concurrently in the same platform. **B-D**.
944 Functional analyses of proteins whose expressions are changed discordantly at total protein and
945 phosphorylation levels. Mitochondria and others are enriched in cellular component analysis (**B**).
946 Functions related to metabolism, mitochondria and others are enriched in Reactome pathway (**C**) and
947 biological process analyses (**D**).

948

949 **Figure 9. Deduced schematic of coordination of phosphoproteome with transcriptome and**
950 **proteome in TGAC8 mouse LV.** Based on our results, we deduced a mechanism of reprogramed
951 phosphoproteome in TGAC8 mouse LV: First, TGAC8 mouse induces a PKA dependent phosphorylation
952 via AC8-cAMP-PKA axis. Many cytoplasmic proteins including TFs are thus phosphorylated and then
953 transported into the nuclear where TFs recognize and bind to the promotors to activate the transcription of

954 more regulatory factors, including kinases, phosphatases, and TFs. The activation states of these factors
955 are changed upon phosphorylated in cytosol, thereby activating additional kinases-controlled
956 phosphorylation cascades and reprogramming the cardiac phosphoproteome comprehensively. Left
957 column: AC8-cAMP-PKA signaling; middle column: phosphorylation (phosphoproteome); lower right:
958 transcription (transcriptome); upper right: translation (proteome).

959

960 **Figure 10. Reprogrammed concentric performance and protection circuitry in response to the**
961 **constitutive challenge of marked cardiac-specific overexpression of adenylyl cyclase type 8.** Based
962 on the present phosphoproteome, we optimized our previously deduced mechanism graph and labeled
963 findings from the phosphoproteome using red stars. TGAC8 mouse induces a chronic cardiac exercise on
964 heart, manifested as increased heart rate and contractility accompanied with increased energy demand and
965 cardiac biomass. Multiple signaling pathways, related to nutrient sensing, energy production, cardiac
966 cellular stress, cardiac stress response, growth factor signaling, and cell proliferation, are potential
967 downstream mediating the effect of the activated AC8-cAMP-PKA-Ca^{2+} signaling in mouse LV. The
968 altered cardiac functions were also observed associated with protein phosphorylation in our previous
969 study and labeled in blue star here.

970

971

972 **Supplementary Figure Legends**

973 **Supplementary Figure 1. The enriched pathway, Cardiac Hypertrophy Signaling (Enhanced), from**
974 **the phosphoproteome.** Cardiac Hypertrophy Signaling (Enhanced) is visualized using IPA. Dots with
975 purple outline are identified phosphoproteins or protein complexes. Red and green fill colors indicate
976 upregulation and downregulation respectively.

977

978 **Supplementary Figure 2. The regulatory pathway under the control of a predicted upstream**
979 **kinase, PDPK1.** PDPK1 in the center is one representative of predicted upstream kinases. Surrounding
980 dots represent identified phosphoproteins differentially regulated in phosphoproteome. Meanings of
981 colors refer to the box of prediction legend besides the graph. Blue glows represent that the increased
982 phosphorylation levels inhibit the activity of corresponding proteins.

983

984 **Supplementary Figure 3. Phosphopeptide number of substrates of PI3K.** Y-axis represents protein
985 substates of PI3K; x-axis represents number of phosphopeptides. Red and blue bars indicate upregulated
986 and downregulated phosphopeptides respectively; green bars indicate nonsignificantly regulated ones. A-
987 B. Red (up): p-value < 0.1 and log2(fold change) > 0; blue (down): p-value < 0.1 and log2(fold change) $>$
988 0; green (ns): p-value ≥ 0.1 or log2(fold change) $= 0$. C. Red (up): p-value < 0.05 and log2(fold change) $>$
989 0; blue (down): p-value < 0.05 and log2(fold change) > 0; green (ns): p-value ≥ 0.05 or log2(fold change)
990 $= 0$.

991

992 **Figures and Supplementary Figures**

993 **Figure 1. TGAC8 reprograms the LV phosphorylation state.**

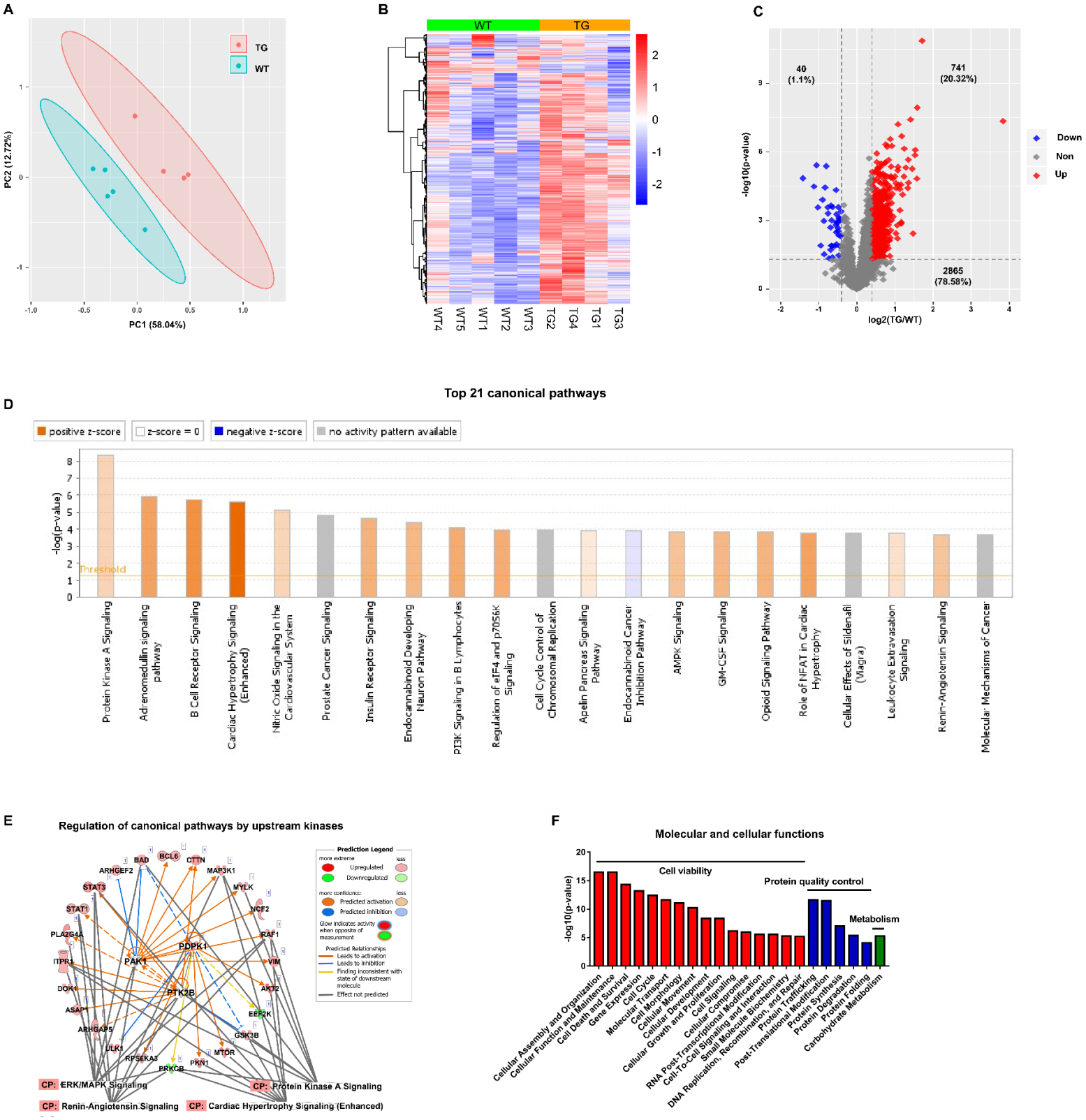

995 **Figure 2. Characteristics of upregulated phosphopeptides.**

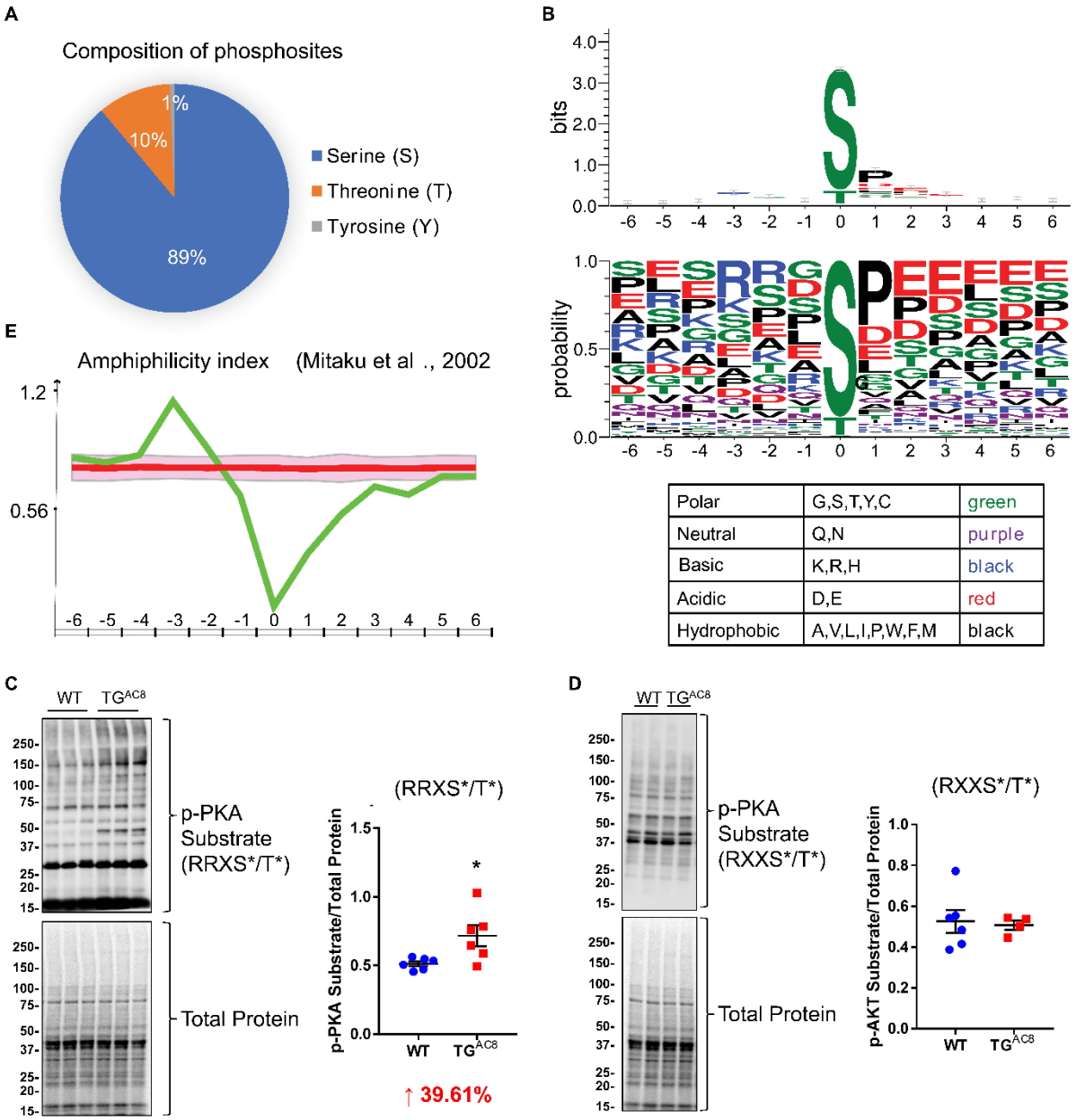

996

997

998

999

1000

1001

1002

1003

Figure 3. Integrative analysis of transcriptome, proteome and phosphoproteome.

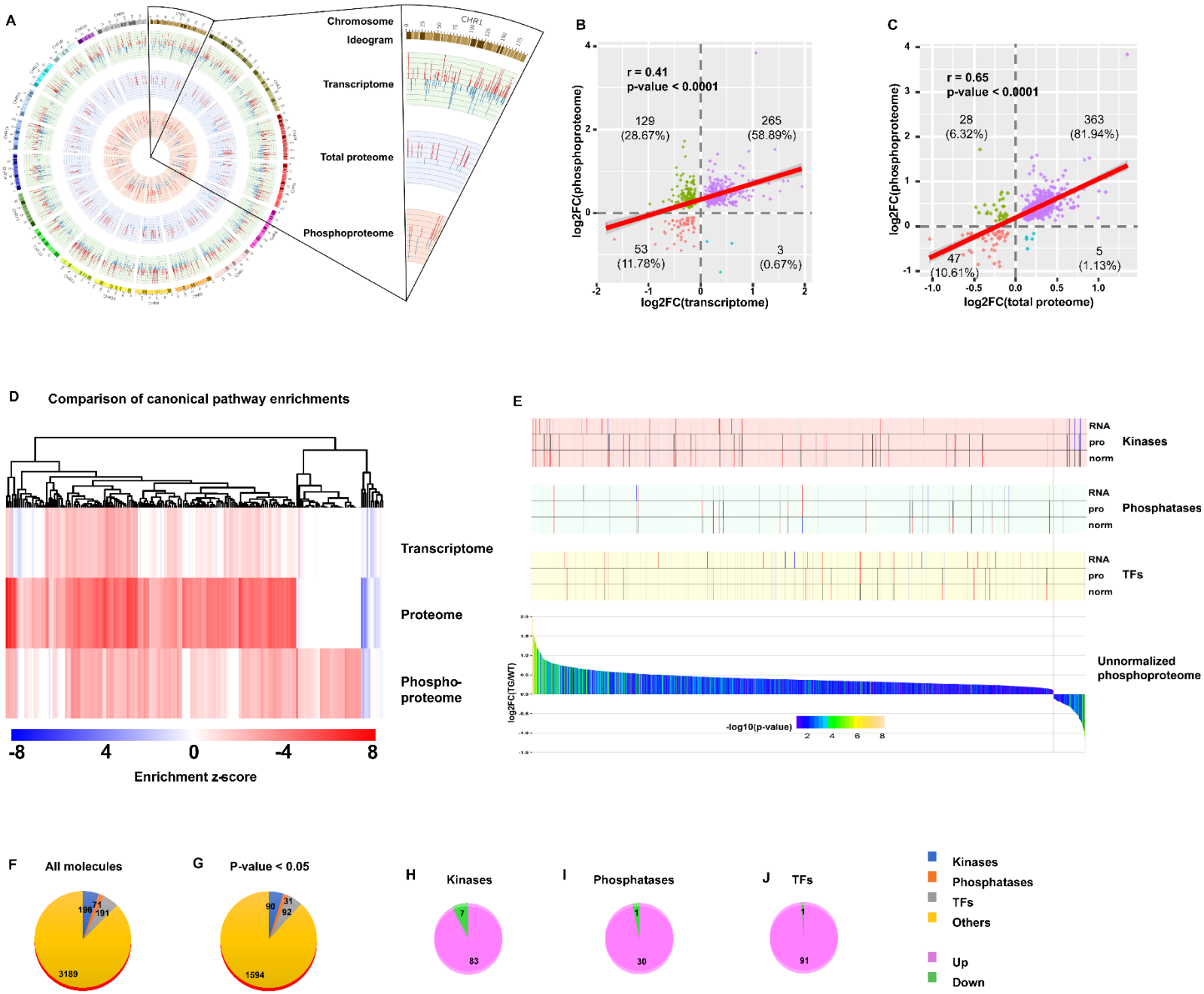

1011 **Figure 4. Coordination of phosphoproteome and transcriptome.**

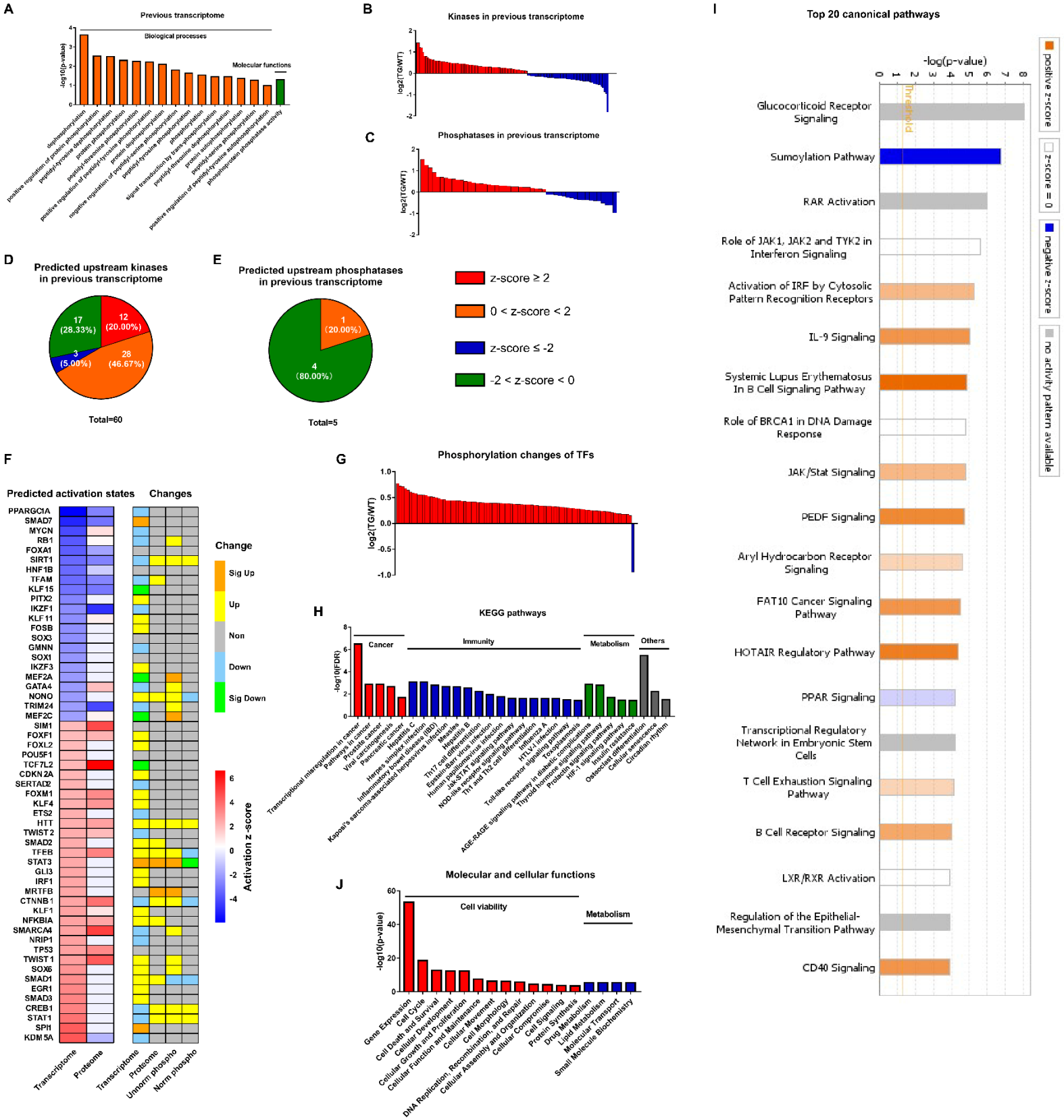

1013 **Figure 5. Analysis of normalized phosphoproteome.**

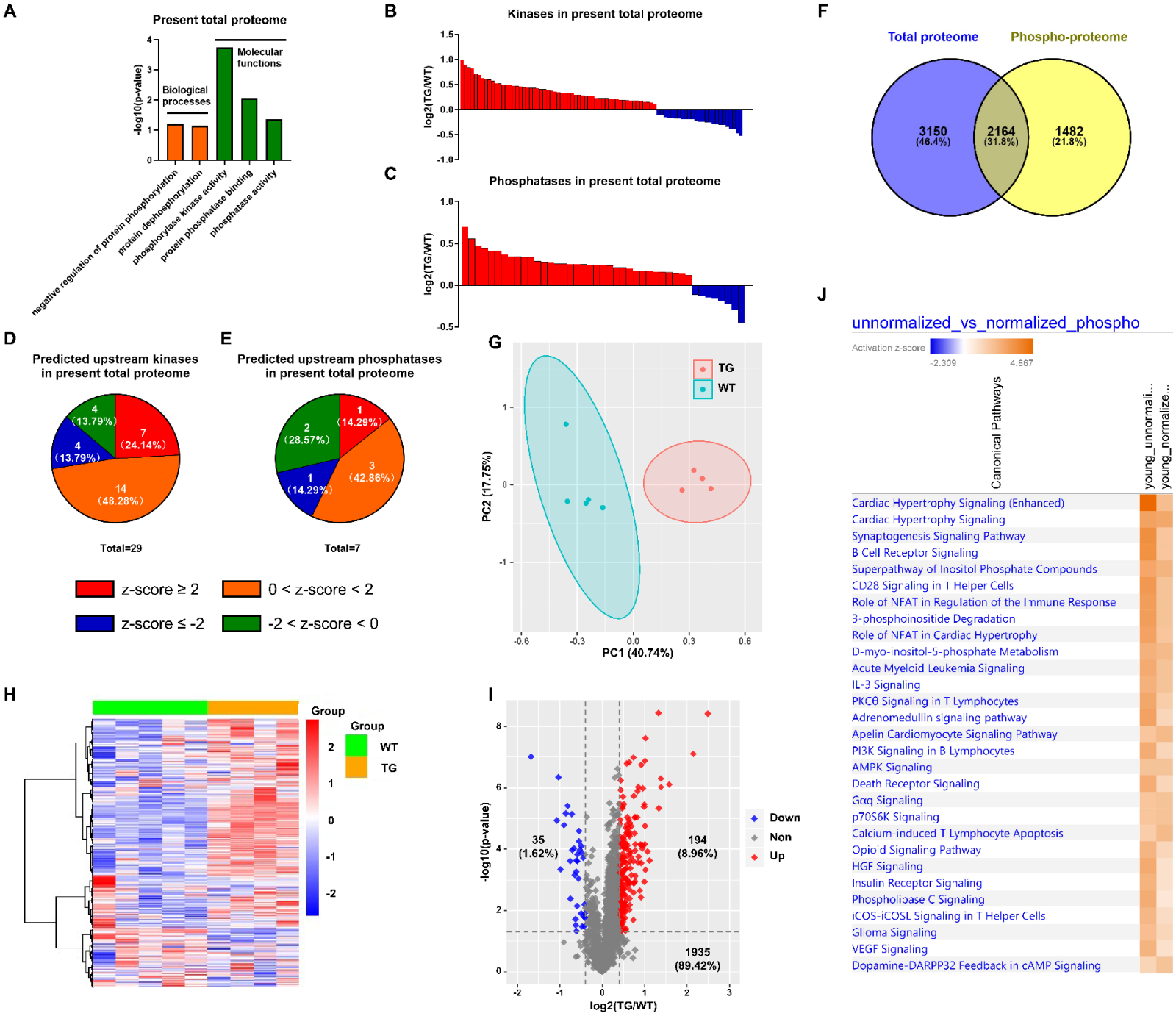

1015

1016

1017

1018

Figure 6. Coordinated regulation of transcriptome, proteome and phosphoproteome on PI3K/AKT and ERK/MAPK signaling pathways and protein synthesis and degradation.

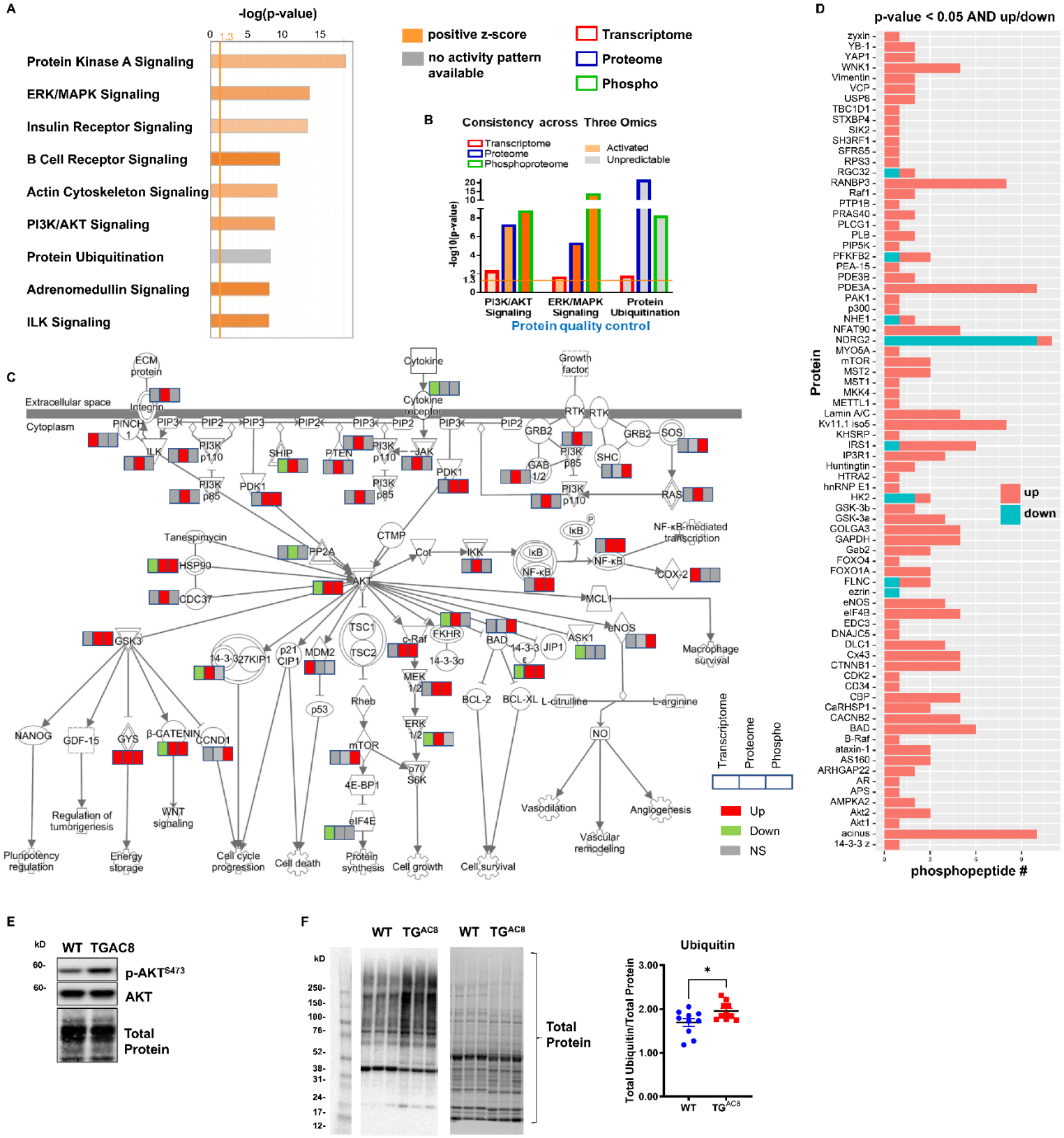

1022 **Figure 7. Cross verification of activated PI3K/AKT and ERK/MAPK signaling pathways and**
1023 **enhanced protein synthesis and degradation from our previous study.**

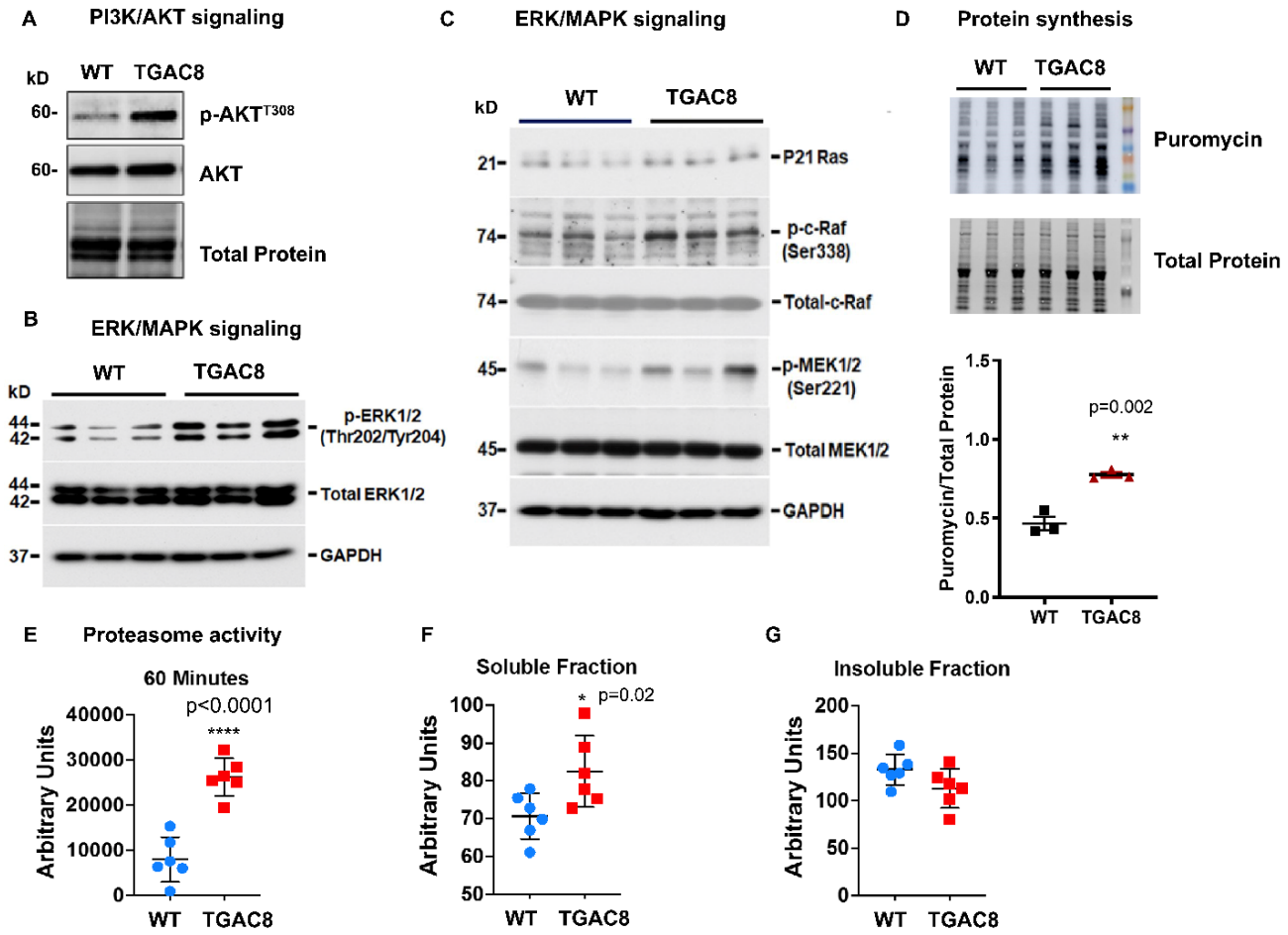

1024
1025
1026
1027
1028
1029
1030
1031
1032
1033
1034
1035

1036 **Figure 8. Analyses of proteins changed discordantly in proteome and phosphoproteome.**

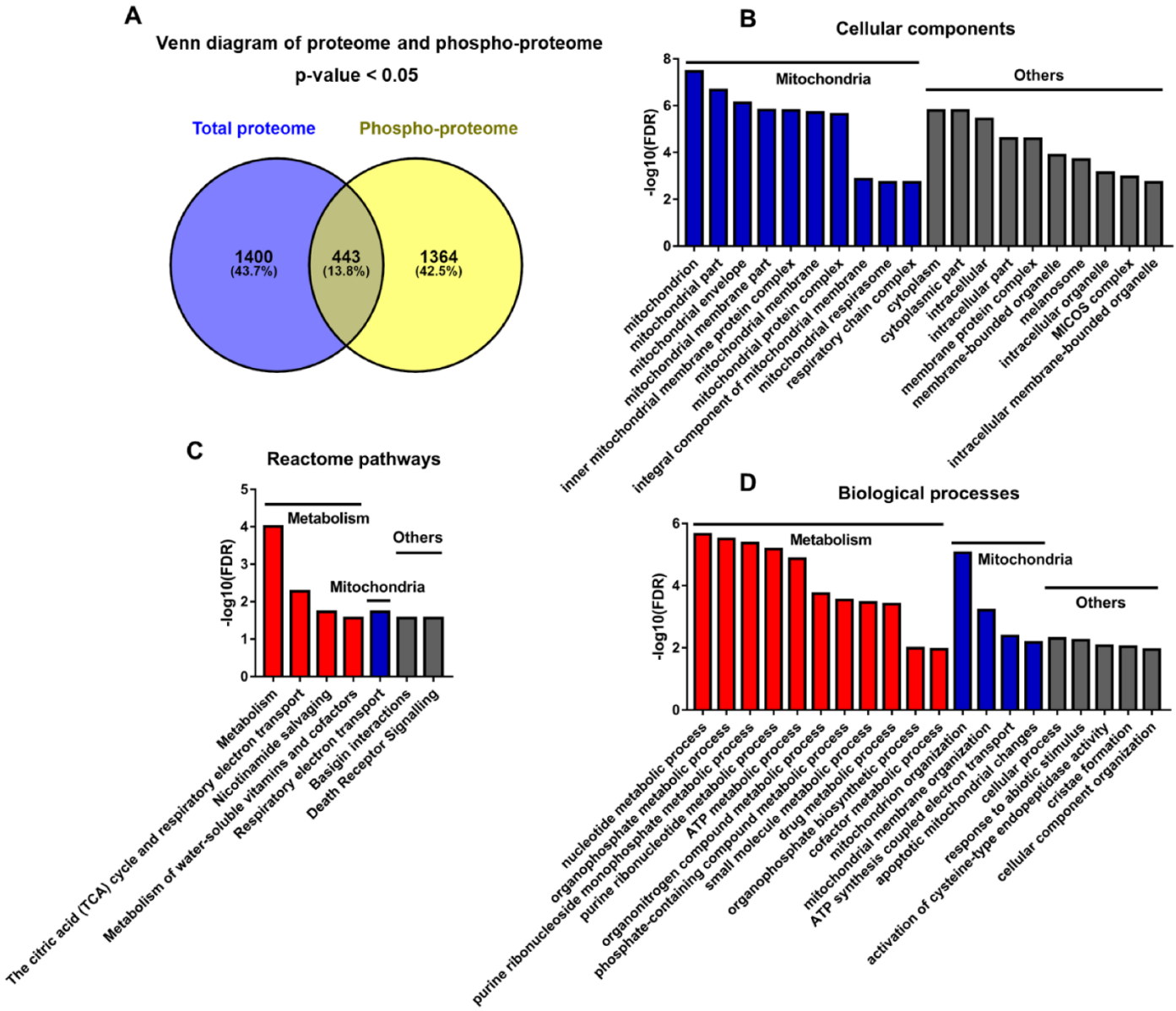

1038

1039

1040

1041

1042

1043

1044

1045 **Figure 9. Deduced schematic of coordination of phosphoproteome with transcriptome and**
1046 **proteome in TGAC8 mouse LV.**

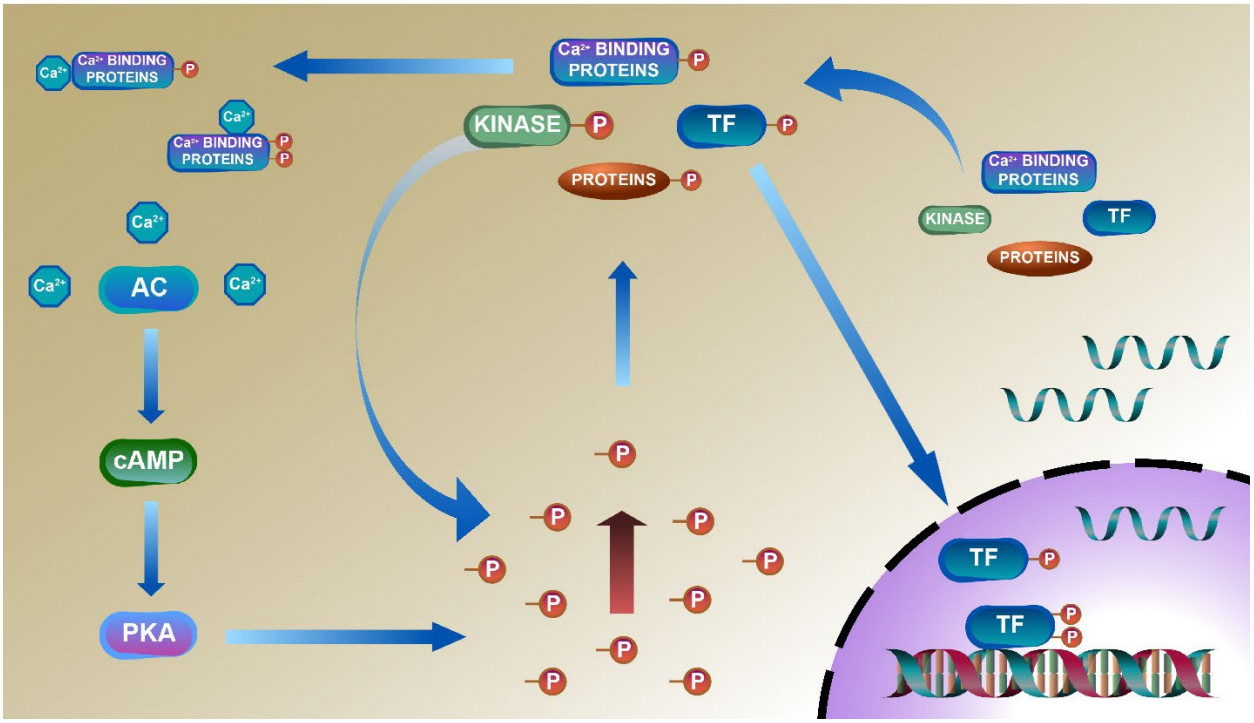

1047

1048

1049

1050

1051

1052

1053

1054

1055

1056

1057

1058

1059

1060

1061

1062

1063 **Figure 10. A comprehensive circuitry of TGAC8 mouse heart concluded from this**
1064 **phosphoproteome combine with previous transcriptome and proteome.**

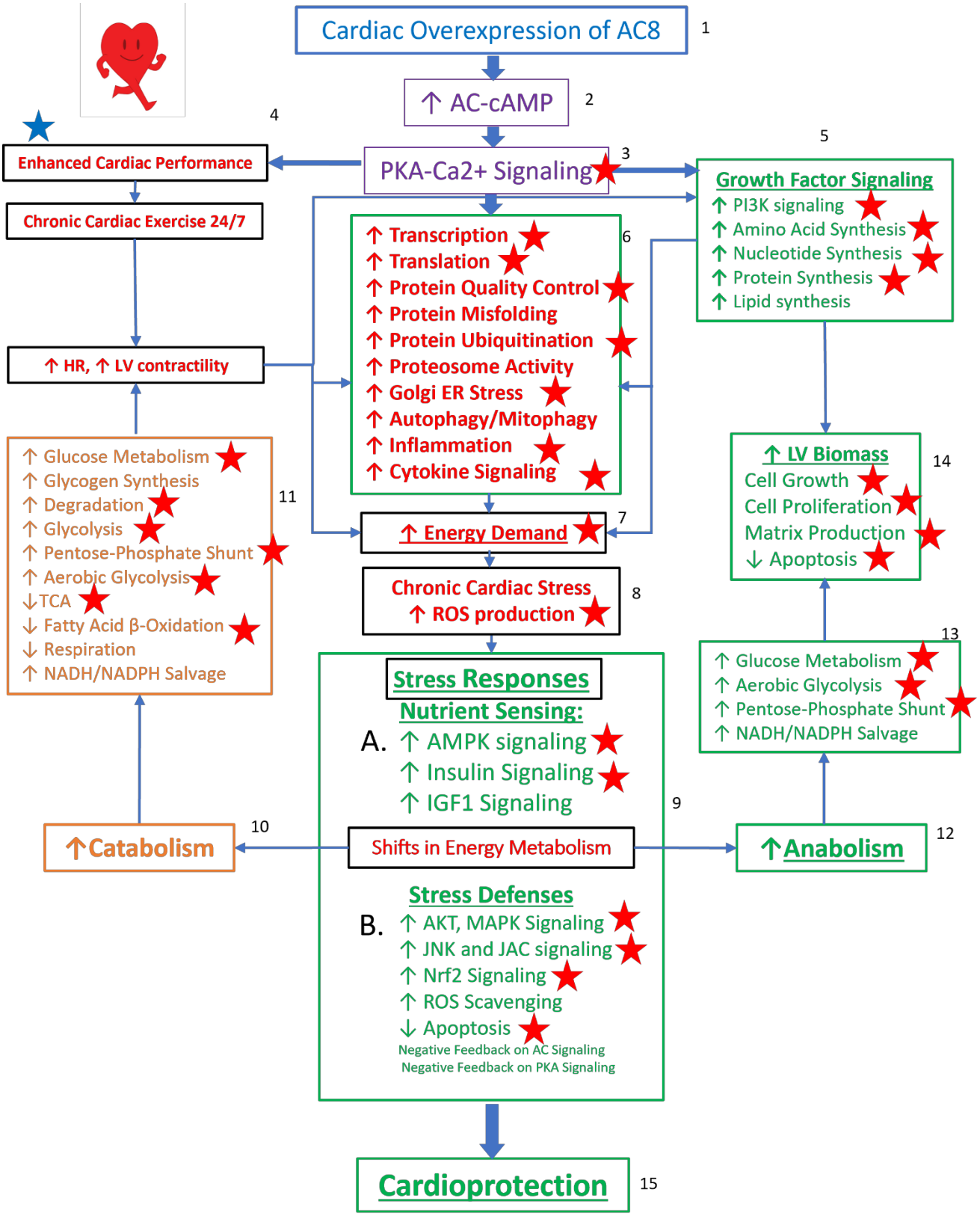

1065

1066 **Supplementary Figure 1. The enriched pathway, Cardiac Hypertrophy Signaling (Enhanced), from the**
1067 **phosphoproteome.**

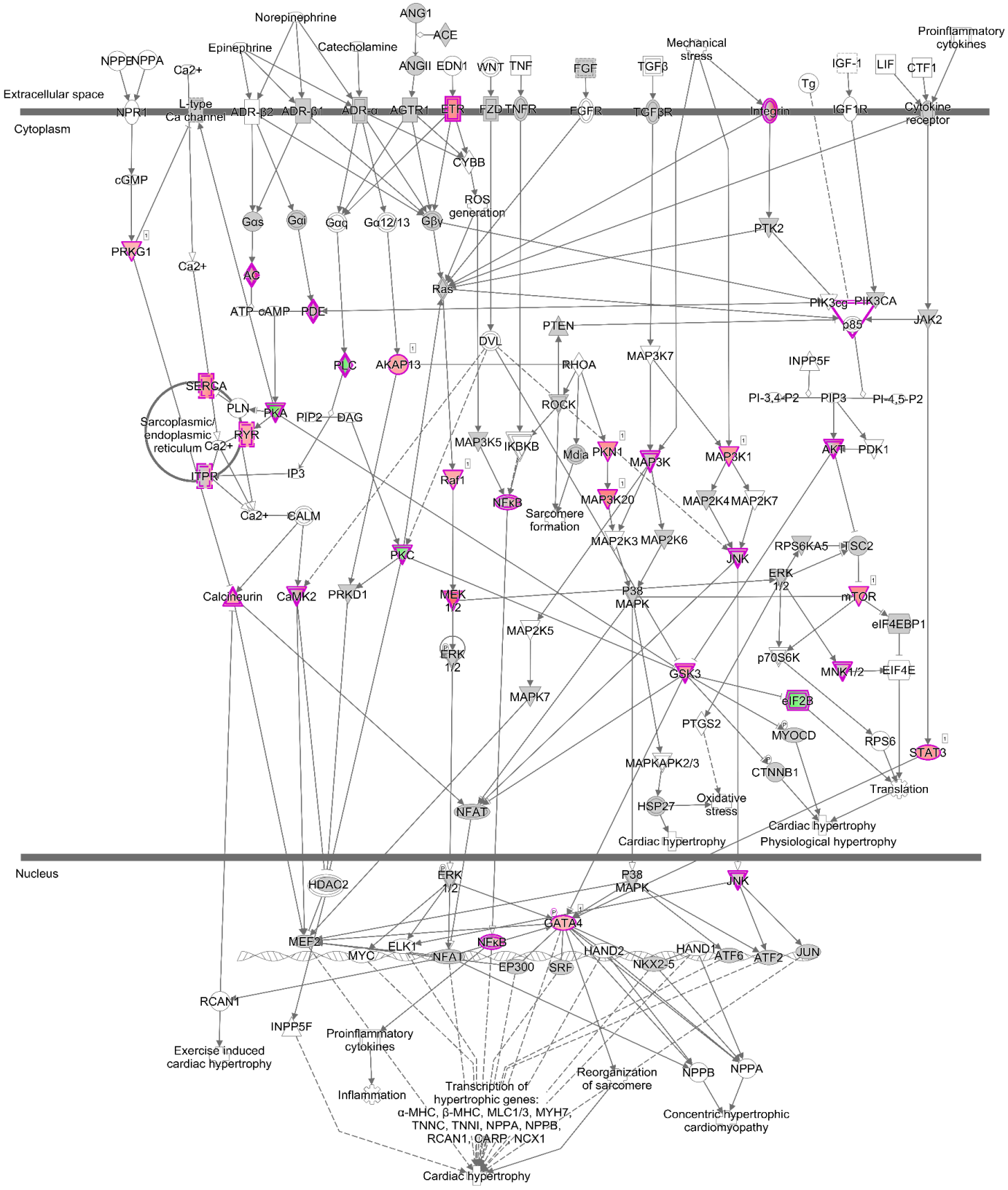

10

1069 **Supplementary Figure 2. The regulatory pathway under the control of a predicted upstream**
1070 **kinase, PDPK1.**

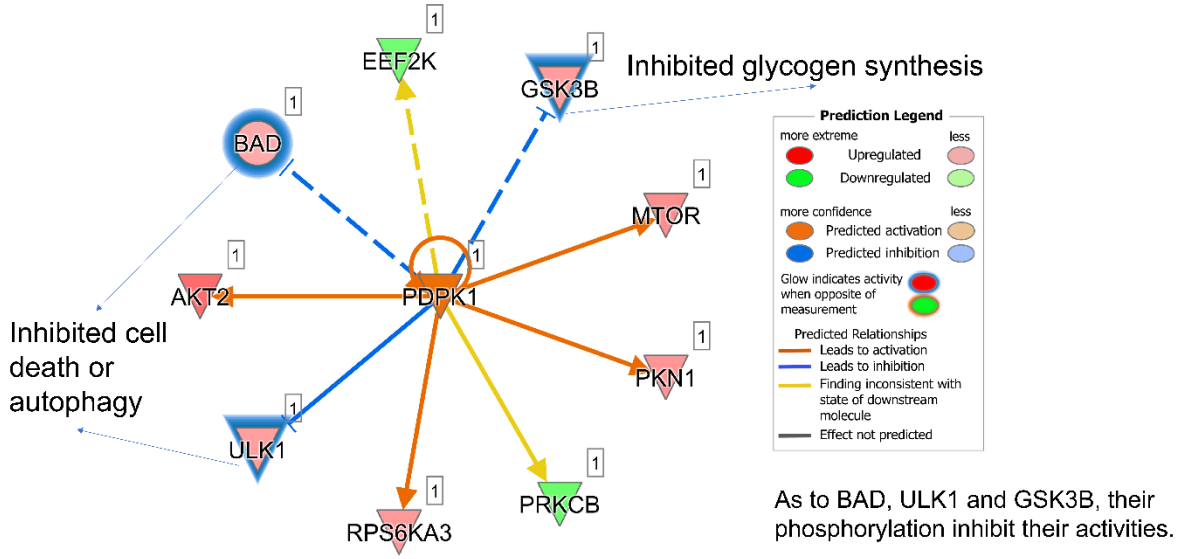

Symbol	Entrez Gene Name	UniProt	Log Ratio	p-value	Location	Family
AKT2	AKT serine/threonine kinase 2	Q60823	0.840825	0.007813	Cytoplasm	kinase
BAD	BCL2 associated agonist of cell death	Q61337	0.476462	7.81E-06	Cytoplasm	other
EEF2K	eukaryotic elongation factor 2 kinase	O08796	-0.42591	0.004744	Cytoplasm	kinase
GSK3B	glycogen synthase kinase 3 beta	Q9WV60	0.556065	0.002741	Nucleus	kinase
MTOR	mechanistic target of rapamycin kinase	Q9JLN9	0.640641	0.000144	Nucleus	kinase
PDPK1	3-phosphoinositide dependent protein kinase 1	Q9Z2A0	0.651174	0.02451	Cytoplasm	kinase
PKN1	protein kinase N1	P70268-2	0.600171	0.007485	Cytoplasm	kinase
PRKCB	protein kinase C beta	P68404-2	-0.44609	0.001011	Cytoplasm	kinase
RPS6KA3	ribosomal protein S6 kinase A3	P18654	0.580733	0.005794	Cytoplasm	kinase
ULK1	unc-51 like autophagy activating kinase 1	O70405	0.549454	0.015177	Cytoplasm	kinase

1071
1072
1073
1074
1075
1076
1077
1078
1079
1080
1081
1082
1083

1084 **Supplementary Figure 3. Phosphopeptide number of substrates of PI3K.**

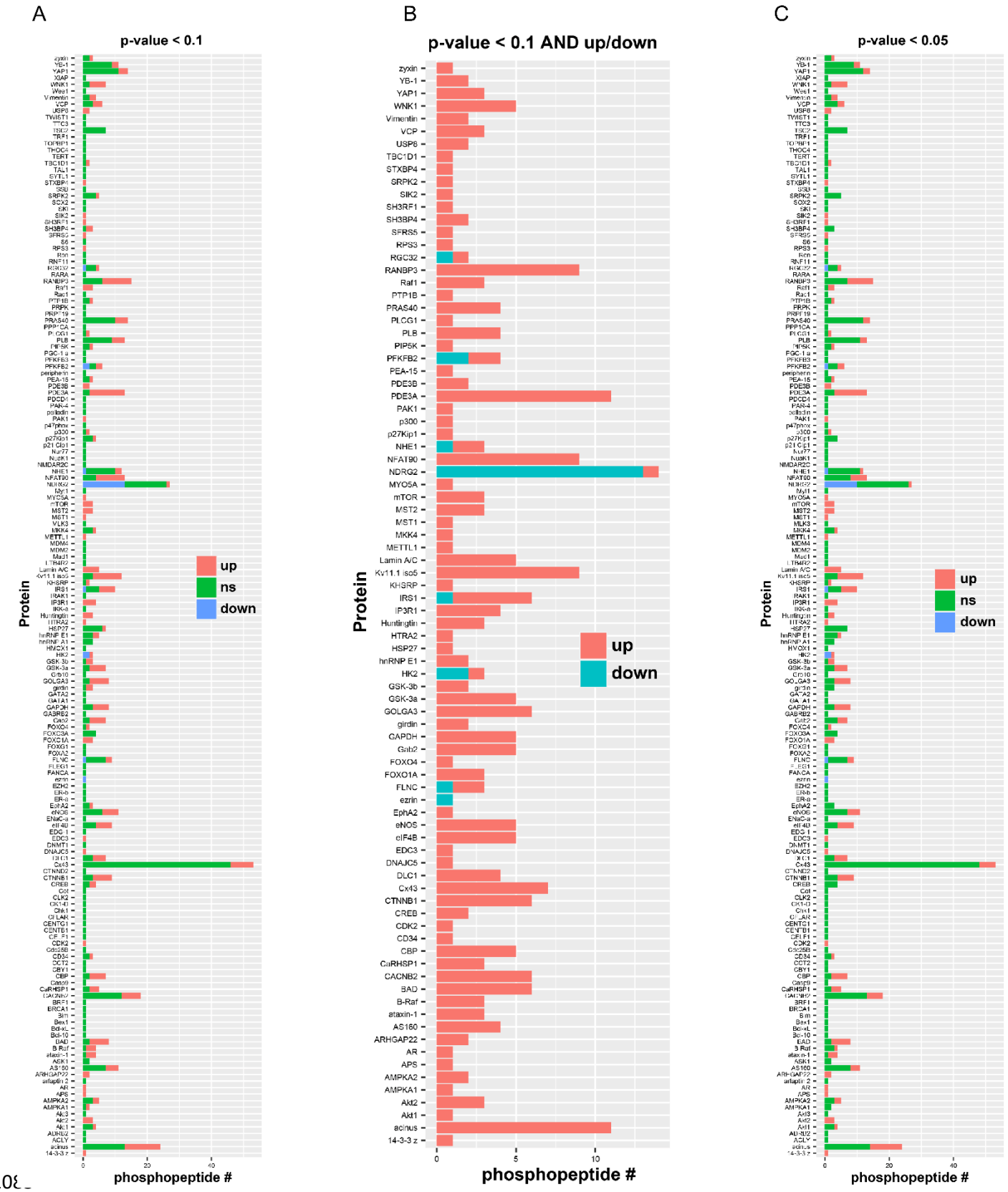

1085